

Full Compositional Flexibility in the Preparation of Mesoporous MFI Zeolites by Desilication

Journal Article

Author(s):

Verboekend, Danny; Mitchell, Sharon; Milina, Maria; Groen, Johan C.; Pérez-Ramírez, Javier

Publication date:

2011-07-28

Permanent link:

<https://doi.org/10.3929/ethz-a-010788858>

Rights / license:

[In Copyright - Non-Commercial Use Permitted](#)

Originally published in:

The Journal of Physical Chemistry C 115(29), <https://doi.org/10.1021/jp201671s>

Funding acknowledgement:

134572 - A fundamental approach to the scale up of hierarchical zeolite catalysts (SNF)

1
2
3
4
5
6
7
8
9
10
11
12
13
14
15
16
17
18
19
20
21
22
23
24
25
26
27
28
29
30
31
32
33
34
35
36
37
38
39
40
41
42
43
44
45
46
47
48
49
50
51
52

Full Compositional Flexibility in the Preparation of Mesoporous MFI Zeolites by Desilication

Danny Verboekend,[†] Sharon Mitchell,[†] Maria Milina,[†] Johan C. Groen,[‡] and Javier Pérez-Ramírez^{†}*

[†] Institute for Chemical and Bioengineering, Department of Chemistry and Applied Biosciences, ETH Zurich, HCI E 125, Wolfgang-Pauli-Strasse 10, CH-8093, Zurich, Switzerland.

[‡] Delft Solids Solutions B.V., Rotterdamseweg 183c, 2629 HD Delft, the Netherlands.

* Corresponding author. Fax: +41 44 633 14 05; E-mail: jpr@chem.ethz.ch.

Abstract

1
2
3 We demonstrate that desilication in alkaline medium is a suitable post-synthetic method to introduce
4
5 intracrystalline mesoporosity in MFI zeolites independent of the Si/Al ratio in the parent material. By
6
7 systematic screening of the influence of both base concentration (0.1-1.8 M NaOH) and Si/Al ratio (10-
8
9 1000) on the properties of the treated zeolites, we reveal that effective mesoporosity introduction
10
11 (>200 m² g⁻¹) may be achieved in the Si/Al range of 12-200. The use of descriptors like the ‘indexed
12
13 hierarchy factor’ and the ‘desilication efficiency’ enable the rational categorization of the solids
14
15 obtained. The highest desilication efficiencies, estimated by correlating the introduced mesoporosity
16
17 with the yields after NaOH treatment, are obtained in the previously established Si/Al range of 25-50.
18
19 We identify the crucial role of a subsequent acid treatment for removing amorphous Al-rich debris from
20
21 alkaline-treated samples in the case of low Si/Al ratios (< 20). The latter acid wash uncovers the
22
23 complete micro- and mesopore network, enabling full compositional flexibility of desilication. The
24
25 removal of the Al-rich debris concomitantly enabled restoration of both the acidity and the chemical
26
27 composition of the hierarchical zeolite to that of the starting (purely microporous) zeolite. Catalytic
28
29 evaluation of selected Al-rich zeolites, as demonstrated in the toluene alkylation with benzyl alcohol,
30
31 confirmed the superiority of the mesoporous alkaline-treated samples with respect to the parent material.
32
33 Hierarchical ZSM-5 after acid washing stands as the most active sample, which stresses the relevance of
34
35 the additional post-synthesis treatment step.
36
37
38
39
40
41
42
43
44

45 **Keywords:** Hierarchical zeolites; Micro/mesoporous materials; Post-synthesis treatments; Desilication;
46
47 Acid treatment; Catalysis.
48
49
50
51
52
53
54
55
56
57
58
59
60

1. Introduction

The promising properties of hierarchical (mesoporous) zeolites, *i.e.* those combining the intrinsic microporosity with an auxiliary network of mesopores, have sparked intense effort to improve the zeolite utilization in catalysis.¹⁻⁴ Among the numerous methods available to prepare mesoporous zeolites, desilication by alkaline treatment is one of the most widely applied, established as a simple and effective approach.^{5,6} Furthermore, the increasing number of zeolite families, prepared in hierarchical form by alkaline treatment (MFI⁷, MTW,⁸ MOR,⁹ BEA,¹⁰ AST,¹¹ FER,¹² MWW,¹³ IFR,¹⁴ STF,¹⁵ CHA,¹⁶ FAU,¹⁷ and TON¹⁸) highlights its versatility.

Pioneering work on desilication was performed by Groen *et al.*,^{19,20} who identified, by applying NaOH treatment on MFI zeolites at a fixed condition, that a confined molar framework Si/Al window (25-50) for optimal intracrystalline mesopore formation exists. At higher Si/Al ratios, uncontrolled silicon extraction occurs, resulting in the formation of larger pores. For low Si/Al ratios, silicon extraction is hampered resulting in limited extra mesoporosity. Consequently, framework aluminum was coined as ‘pore-directing agent’ (PDA), due to its regulatory effect on silicon leaching. Apart from Al³⁺, other trivalent heteroatoms in lattice positions (Fe³⁺, Ga³⁺, B³⁺) also proved successful in exerting the role of PDA.²¹ Several routes to tune the desilication process over zeolites within the optimal range have been reported, *e.g.* partial detemplation-desilication,²² the application of microwave irradiation,²³ and the use of alternative bases^{24,25} or pore-growth moderators.²⁶ Additionally, by combining alkaline with steam²⁷ or acid²⁸ treatments, the mesopore formation was decoupled from acidity modification.

Apart from optimization of the desilication treatment, significant progress concerning the in-depth characterization and categorization of hierarchical zeolites has been achieved. For example, the accessibility index (ACI)²⁹ provides a powerful tool to standardize acid site accessibility in zeolites, while the hierarchy factor (HF)²⁶ couples the developed mesoporosity to the preserved intrinsic microporosity. More specifically for alkaline leaching, the ‘desilication efficiency’ was recently introduced in consideration of the zeolite weight loss incurred upon introduction of mesoporosity.¹⁸

1
2
3
4
5
6
7
8
9
10
11
12
13
14
15
16
17
18
19
20
21
22
23
An important advance in the preparation of mesoporous all-silica zeolites by desilication, was the use of external PDAs, such as tetraalkylammonium cations or metal complexes. The deliberate addition of PDAs to the alkaline solution enabled the preparation of mesoporous silicalite-1.³⁰ In addition to expanding the range of feasible Si/Al ratios to infinity, this work demonstrated that the pore-directing action is executed at the external surface of the zeolite. The latter implies that framework aluminum (or any other trivalent cation) does not play a direct pore-directing role. Instead, only aluminum extracted from the framework actively participates in pore formation; by an ‘alkaline-induced alumination’ of the external surface. In conclusion, three major factors were identified to govern the formation of intracrystalline mesoporosity: (i) the zeolite, (ii) the treatment conditions, and (iii) the presence of PDAs.

24
25
26
27
28
29
30
31
32
33
34
35
36
37
38
39
40
41
42
43
44
The final hurdle to achieve full compositional flexibility in the preparation of mesoporous zeolites by desilication requires tackling the low Si/Al range. To date, mesoporous Al-rich MFI zeolites are mostly prepared *via* a different approach, *e.g.* by carbon templating,³¹ or by altering the composition to within the optimal window by dealumination prior to alkaline treatment.³² Though, in the latter case, the mesoporous zeolite no longer comprises an Al-rich framework. Strikingly, although the literature suggests that alkalinity is of critical importance,⁸ the impact of base concentration on mesoporosity development in low Si/Al ratio zeolites has not been systematically explored. Previous studies varying alkalinity have primarily focused on individual zeolites of Si/Al ratios within or near the preferred range (25-50), adjusting according to either framework structure or morphology.^{7,12,19,33-36}

45
46
47
48
49
50
51
52
53
54
55
56
57
58
59
60
Herein, we provide further insight into the mechanism of mesopore formation in basic media enabling full compositional flexibility in the preparation of hierarchical zeolites. Exploring the entire range of Si/Al ratios in MFI (10-1000), we probe the influence of base concentration on the properties of the treated zeolites. By monitoring changes in yield, crystallinity, and porosity, we map the formation of mesoporous zeolites enabling their purpose design. Descriptors as the indexed hierarchy factor and the desilication efficiency are used to categorize the porous structures obtained and to relate the

mesoporosity developed with the associated weight loss. We show that mesoporous Al-rich zeolites can be prepared by desilication at high base concentrations, leading to an improved performance in toluene alkylation with benzyl alcohol. However, a subsequent acid treatment of the alkaline-treated samples is of paramount importance to remove amorphous Al-rich debris thereby uncovering the entire micro- and mesopore network. The acid treatment enables to restore both the Si/Al ratio and the acidity, and further enhances the catalytic activity.

2. Experimental

2.1. Post-synthesis treatments

Various commercial MFI zeolites in ammonium form were used in the post-synthesis treatments: Z10, (PZ2/23, Zeochem), Z15 (CBV 3024E, Zeolyst International), Z25 (CBV 5524G, Zeolyst International), Z40 (CBV 8014, Zeolyst International), and Z1000 (HSZ-890H0A, Tosoh Corporation). The number in the Z_x code refers to the Si/Al ratio according to manufacturer's specifications. The parent zeolites (code P) were obtained by calcination of the as-received powders by heating to 823 K at 5 K min⁻¹ and thermal treatment for 5 h in static air. Alkaline treatments were carried out in 0.10-1.8 M aqueous NaOH (3.3 g of zeolite per 100 cm³ of solution) using an EasymaxTM 102 reactor system from Mettler Toledo. In a typical experiment, the alkaline solution was stirred at 500 rpm and heated to 338 K, after which the parent zeolite sample was introduced. The resulting suspension was left to react for 30 min, followed by quenching, filtration, extensive washing using distilled water, and overnight drying at 338 K. Some samples were subsequently acid treated in 0.02-0.10 M aqueous HCl (1 g zeolite per 100 cm³ of solution) at 338 K for 6 h. Prior to acidity characterization, the zeolites were converted into the protonic form by 3 consecutive ion exchanges in 0.10 M aqueous NH₄NO₃ (298 K, 12 h, 1 g zeolite per 100 cm³ of solution), followed by calcination as described for the parent zeolite. Treated samples were coded 'xNaOH' or 'yHCl', where x and y represent the molarity of NaOH and HCl solutions, respectively.

2.2. Characterization

N₂ isotherms were measured in a Quantachrome Quadrasorb-SI gas adsorption analyzer at 77 K. Samples were degassed in vacuum at 573 K for 10 h prior to measurement. The total pore volume was derived from the amount of N₂ adsorbed at $p/p_0 = 0.99$ and the t -plot method³⁷ was used to discriminate between micro- and mesoporosity. The Brunauer-Emmett-Teller (BET) method³⁸ was applied to determine the total surface area (S_{BET}), which is used for comparative purposes. The mesopore size distribution was obtained by applying the Barrett-Joyner-Halenda (BJH) method³⁹ to the adsorption branch of the isotherm.

X-ray diffraction (XRD) was undertaken using a PANalytical X'Pert PRO-MPD diffractometer equipped with Bragg-Brentano geometry and Ni-filtered Cu K α radiation ($\lambda = 0.1541$ nm). Data were recorded in the range 5-50° 2θ with an angular step size of 0.05° and a counting time of 8 s per step. Samples were ground to minimize the effects of preferred orientation and supported on a flat specimen holder, with a fixed sample volume irradiated by the X-ray beam. The variation in zeolite crystallinity resulting from post-synthetic modification was derived from the relative intensity of the intense (051) reflection at 23° 2θ , assuming 100% crystallinity in the parent sample. The reproducibility of the crystallinity analysis was within 1%.

The Si and Al content in selected solids and filtrates collected after alkaline and acid treatment, were analyzed by atomic absorption spectroscopy (AAS) in a Varian SpectrAA 220 FS spectrometer.

Transmission electron microscopy (TEM) imaging was performed with a Phillips CM12 instrument operated at 100 kV.

Magic angle spinning nuclear magnetic resonance (MAS NMR) spectra were recorded at a spinning speed of 8 kHz on a Bruker Avance 700 NMR spectrometer equipped with a 4 mm probe head and 4 mm ZrO₂ rotors at 182.4 MHz. ²⁷Al spectra were recorded using 2048 accumulations, 90° pulses with a pulse length of 2.4 μ s, a recycle delay of 0.25 s, and (NH₄)Al(SO₄)₂·12H₂O as the reference. ²⁹Si

1 spectra were acquired using 2048 accumulations, 90° pulses with a pulse length of 12.5 μs, a recycle
2 delay of 10 s, and 2,2-dimethyl-2-silapentane-5-sulfonic acid as the reference.
3

4
5 Infrared spectroscopy was performed under a N₂ atmosphere at 473 K using a Thermo Nicolet 5700
6 spectrometer equipped with a SpectraTech Collector II diffuse reflectance accessory and a high-
7 temperature cell. Prior to the measurement, the sample was dried at 573 K in N₂ flow (100 cm³ min⁻¹)
8 for 60 min. Spectra were recorded in the range of 650-4000 cm⁻¹ with a nominal resolution of 4 cm⁻¹ and
9 co-addition of 200 scans.
10
11

12
13
14
15
16
17 Temperature-programmed desorption of ammonia (NH₃-TPD) was carried out in a Thermo TPDRO
18 1100 unit equipped with a thermal conductivity detector. The zeolite (100 mg) was pretreated at 823 K
19 in He flow (20 cm³ min⁻¹) for 2 h. Afterwards, 10 vol.% NH₃ in He (20 cm³ min⁻¹) was adsorbed at
20 473 K for 30 min followed by He purging at the same temperature for 1 h. This procedure was repeated
21 three times. Desorption of NH₃ was monitored in the range 473-973 K using a ramp rate of 10 K min⁻¹.
22
23
24
25
26
27
28
29
30

31 **2.3. Catalytic measurements**

32
33 The alkylation of toluene with benzyl alcohol was conducted in an Endeavor[®] Catalyst Screening
34 System (Argonaut Technologies), consisting of 8 parallel reactors with a working volume of 5 cm³ and
35 with continuous stirring by overhead impellers. Reaction conditions were $P = 0.5$ MPa, $T = 433$ K,
36 molar toluene-to-benzyl alcohol ratio (T/BA) = 80, and catalyst amount = 40 wt.% of zeolite with
37 respect to the amount of benzyl alcohol. Liquid samples were analyzed at different reaction times using
38 a gas chromatograph (HP 6890) coupled to a mass selective detector (HP 5973).
39
40
41
42
43
44
45
46
47
48
49

50 **3. Results and discussion**

51 **3.1. Two-dimensional screening of desilication**

52
53 Alkaline treatments were performed over various commercial MFI zeolites representative of the full
54 Si/Al range for MFI, *i.e.* Z10, Z15, Z25, Z40, and Z1000. ²⁷Al MAS NMR evidenced that the parent
55
56
57
58
59
60

1 zeolites contained predominantly tetrahedral Al (band at 59 ppm), ascribed aluminum in framework
2 positions (Figure SII). Additionally, some octahedrally-coordinated Al (band at 0 ppm), attributed to
3 extra-framework aluminum, was demonstrated. The contribution of the latter species decreased with the
4 Si/Al ratio; in the case of Z10 a significant amount was present, for Z15 and Z25 minor amounts were
5 evidenced, whereas for Z40 and Z1000 no distinguishable contributions appeared. The influence of the
6 extra-framework aluminum in the case of Z10 is discussed in Section 3.2. The temperature (338 K) and
7 time (30 min) of the alkaline treatments were kept constant, while the NaOH concentration was varied
8 between 0.1 and 1.8 M. In Figure 1 selected nitrogen isotherms and corresponding BJH mesopore size
9 distributions illustrate the porous properties of the parent and treated zeolites. Table SII provides a
10 complete overview of parent and treated zeolites. In Figure 2, various contour plots illustrate the
11 variation in yield, crystallinity, and porous properties of the solids derived from the two-dimensional
12 screening. Additionally, two contour plots concern the indexed hierarchy factor, which is explained
13 below.

14
15
16
17
18
19
20
21
22
23
24
25
26
27
28
29
30
31 **Yield, crystallinity, and porosity.** Figure 2a shows that, in line with findings of Čížmek *et al.*,⁴⁰ yields
32 reduced with increasing NaOH concentration and Si/Al ratio of the parent zeolite. The yields for Z40
33 and Z1000 did not differ much due to the relative abundance of Si. On the other hand, for Si/Al < 25,
34 the changes in yields are more pronounced. For example, to obtain a yield of *ca.* 60%, Z15 required an
35 alkalinity substantially higher (0.7 M NaOH) than that for Z25 (0.4 M NaOH). Since upon alkaline
36 treatment, intracrystalline mesopores are formed by selective dissolution, a reduced yield (typically *ca.*
37 60-70%) is a prerequisite to obtain substantial mesopore surface areas.^{18,30} We can therefore deduce
38 that, in order to create intracrystalline mesopores in zeolites of Si/Al ratio < 20, an increased alkalinity
39 is required.

40
41
42
43
44
45
46
47
48
49
50
51
52 Substantial mesopore surfaces areas ($S_{\text{meso}} \geq 200 \text{ m}^2 \text{ g}^{-1}$) were measured for virtually all MFI zeolites
53 studied, emphasizing the wide compositional flexibility of desilication (Figure 2c). The highest values
54 (>300 $\text{m}^2 \text{ g}^{-1}$) were obtained for Z40, whereas the lowest surface areas were obtained at the extremes of
55
56
57
58
59
60

1 the MFI Si/Al spectrum, that is, for Z1000 (maximum $132 \text{ m}^2 \text{ g}^{-1}$) and Z10 (maximum $170 \text{ m}^2 \text{ g}^{-1}$).
2
3 Consequently, the range in which alkaline treatment (using only aqueous NaOH) is able to introduce
4
5 significant mesoporosity in MFI zeolites is much broader (12-200) than that initially cited (25-50).²⁰
6
7 The latter limit appears to be suitable mostly for conditions similar to the 'standard' alkaline treatment
8
9 (0.2 M NaOH, 65°C , 30 min, zeolite-to-liquid ratio = 33 g L^{-1}). For low Si/Al ratios, the highest external
10
11 surface areas are achieved at higher NaOH concentrations, in agreement with the result from [Figure 2a](#).
12
13

14 [Figure 2b](#) shows that the greatest loss of crystallinity occurs for the most mesoporous samples (*e.g.*
15
16 Z40 treated in 0.5 M NaOH), as well as for the zeolites of Si/Al < 25 treated in NaOH concentrations
17
18 exceeding 0.6 M. The relatively small crystallinity loss for Z1000 should be related to the absence of
19
20 substantial mesoporosity, while the strong crystallinity decrease upon desilication of zeolites of low
21
22 Si/Al ratio exposed to high alkaline concentrations is assigned to the presence of both intracrystalline
23
24 mesopores and amorphous debris (*vide infra*).
25
26
27

28
29 A decrease of the micropore volume (V_{micro}) is frequently observed upon NaOH treatment of
30
31 zeolites.^{14,17,18,20,26} [Figure 2d](#) shows that (for MFI) this reduction increases with the Al content of the
32
33 parent zeolite. In the case of Z1000, the reduction of V_{micro} is limited (down to $0.13 \text{ cm}^3 \text{ g}^{-1}$), despite
34
35 extensive dissolution. For Z40 the reduction is more pronounced; especially the more mesoporous
36
37 samples ($S_{\text{meso}} > 300 \text{ m}^2 \text{ g}^{-1}$) display significantly reduced micropore volumes (down to *ca.*
38
39 $0.10 \text{ cm}^3 \text{ g}^{-1}$). A severe reduction of V_{micro} (down to *ca.* $0.03 \text{ cm}^3 \text{ g}^{-1}$) is observed for zeolites with
40
41 Si/Al < 15 treated at NaOH concentrations greater than 0.8 M. In line with previous observations,^{18,41}
42
43 this suggests that the micropore reduction is due to the presence of amorphous Al-rich debris.
44
45
46

47
48 The variations in S_{meso} and V_{micro} are directly reflected in the total BET surface area. [Figure 2e](#) shows
49
50 that the maximum corresponds reasonably to the maximum obtained for the developed S_{meso} (obtained
51
52 for Z40, treated in 0.5 M NaOH). On the other hand, S_{BET} decreases strongly upon reduction of the
53
54 micropore volume (Si/Al < 15, alkalinity > 0.8 M NaOH). Hence, from the total surface area alone one
55
56 can already get an indication of the quality of hierarchical pore systems. Since ideally the introduced
57
58
59
60

1 auxiliary porosity is coupled to a fully preserved microporosity, the total surface area in a superior
2 hierarchical zeolite should be higher than that of its purely microporous analogue.
3

4
5 The total pore volume (V_{pore}) increases with the alkalinity for all zeolites due to the introduction of
6 mesopores (Figure 2f). Similar to the trend in yield and S_{meso} , the highest values are obtained for
7 Si/Al = 40 and Si/Al ratios < 25 require higher alkalinities to obtain an increased V_{pore} . For the latter
8 Si/Al range the maximum total pore volumes are obtained at *ca.* 0.2 M higher molarities compared to
9 the maximum in S_{meso} . This should be due to the greater contribution of large mesopores and
10 macropores to the pore volume than to the mesopore surface.
11
12
13
14
15
16
17
18

19 **Indexed hierarchy factor.** The introduction of mesoporosity in zeolites is frequently coupled to a
20 reduction of the micropore volume.²⁶ With this in mind, the hierarchy factor (HF) was introduced,
21 relating a relative mesoporosity ($S_{\text{meso}}/S_{\text{BET}}$) mesoporosity to a relative microporosity ($V_{\text{micro}}/V_{\text{pore}}$). This
22 factor proved very helpful in rationalizing the entire field of mesoporous zeolites, in particular with
23 respect to the different framework types and preparative approaches. Moreover, relation of the hierarchy
24 factor of mesoporous zeolites with catalytic activity yielded sensible trends in alkylation and pyrolysis
25 reactions.^{14,26} Herein, we introduce a variation of the hierarchy factor that fulfills the same function, but
26 is more sensitive to the method applied and the framework type. The micropore volume of MFI is
27 known (*ca.* 0.16 cm³ g⁻¹) and the maximum amount of mesopore surface area obtained by desilication
28 can be derived from our screening (403 m² g⁻¹, see Table SII). We can therefore normalize both V_{micro}
29 and S_{meso} with respect to their maximum values, *i.e.* $\text{IHF} = (V_{\text{micro}}/V_{\text{micro,max}}) \times (S_{\text{meso}}/S_{\text{meso,max}})$. Since the
30 obtained values are normalized (in this case to MFI and desilication), we have coined this modified
31 version as the ‘indexed hierarchy factor’. Figure 2g shows the indexed hierarchy factor (IHF) as a
32 function of Si/Al ratio and NaOH concentration. The IHF is optimal in the region of highest
33 mesoporosity development (Si/Al = 40, 0.5 M NaOH). In fact, the contour plot follows very much the
34 pattern of S_{meso} . The only noticeable difference comprises Si/Al < 15 treated at concentrations of 0.9 to
35 1.2 M; in this area the remarkable drop in microporosity leads to lower values. When the IHF is
36
37
38
39
40
41
42
43
44
45
46
47
48
49
50
51
52
53
54
55
56
57
58
59
60

1 extended to take into account the zeolite loss, by factoring the IHF by the yield, a similar pattern is
2 observed, but shifted to lower NaOH concentrations (Figure 2h). The shift is more pronounced for
3 zeolites with Si/Al > 40, due to the sharp dependence of the yield on the alkalinity. The importance of
4 the yield is further illustrated below.
5
6
7
8

9 **Desilication efficiency.** With an open eye to industrialization, we examine the degree of zeolite
10 dissolution upon introducing external surface area in more detail. The descriptor ‘desilication
11 efficiency’ was recently developed, relating the increase in mesopore surface area to the weight loss
12 upon desilication.¹⁸ Figure 3a shows the increase in mesopore surface area (ΔS_{meso}) plotted against the
13 weight loss upon alkaline treatment of Z10, Z15, Z40, and Z1000. It should be noted that the external
14 surface area present in the parent sample is typically derived from mostly intercrystalline mesopores,
15 whereas the alkaline-treated samples comprise mostly intracrystalline mesopores. This suggests that, in
16 some cases, the ΔS_{meso} may underestimate the introduced intracrystalline mesopore surface area. The
17 data points in Figure 3a correspond to zeolites treated with 0.1-1.0 M NaOH. A linear correlation is
18 observed in all cases, albeit with a different slope. This slope ($dS_{\text{meso}}/d(\text{weight loss})$), is defined as the
19 desilication efficiency, and depends strongly on the Si/Al ratio. In the case of Z40 the mesopore surface
20 increases by *ca.* $4.5 \text{ m}^2 \text{ g}^{-1}$ per percent of weight loss (hereafter $\text{m}^2 \text{ g}^{-1} \%^{-1}$). Concerning Z15, the
21 mesopore surface increases by *ca.* $3 \text{ m}^2 \text{ g}^{-1} \%^{-1}$. For Z10 and Z1000 the desilication efficiency is limited
22 to *ca.* $1 \text{ m}^2 \text{ g}^{-1} \%^{-1}$. Figure 3b compares the desilication efficiencies with respect to the Si/Al ratio of the
23 parent zeolites, resulting in a volcano plot centered around Si/Al = 40. Hence, from Figure 3 we
24 conclude that the preparation of hierarchical zeolites by alkaline treatment is (i) most effective (largest
25 external surface) and (ii) most efficient (smallest relative weight loss) for zeolites with Si/Al ratio in the
26 range of 25-50. The lower desilication efficiencies obtained at the extremes of the compositional Si/Al
27 spectrum are attributed to differences in the mechanism of zeolite dissolution. In the absence of Al
28 (Z1000), the development of mesoporosity is hampered due to the more unselective dissolution. In the
29 case of zeolites with low Si/Al ratio (Z10, Z15), a reduced efficiency arises due to the impeding effect
30
31
32
33
34
35
36
37
38
39
40
41
42
43
44
45
46
47
48
49
50
51
52
53
54
55
56
57
58
59
60

of Al-rich debris. The latter aspect is detailed in Section 3.2.

3.2. Desilication of low Si/Al ratio MFI zeolites

Introduction of mesoporosity by alkaline treatment. Desilication aimed at introducing mesoporosity in MFI zeolites with low Si/Al ratio zeolites is relatively unexplored. This study investigates the introduction of mesoporosity in these zeolites using alkaline solutions of increasing NaOH concentration. We focused particularly on the preparation of mesoporous Z15.

N₂ adsorption performed on the parent Z15 resulted in a type I isotherm characteristic of conventional mostly microporous zeolites (Figures 1b,c). Not uncommon to commercial zeolites, the parent material revealed a considerable S_{meso} (76 m² g⁻¹, Table SII). The BJH mesopore distribution did not show intracrystalline mesopores, and TEM (Figure 4) confirmed that the external surface area is attributable to intercrystalline voids. Additionally, a micropore volume of 0.14 cm³ g⁻¹ was evidenced.

Upon contacting the parent with solutions of increasing alkalinity yields gradually decreased (down to 20% at 1.8 M NaOH), indicating a more extensive zeolite dissolution (Figure 5a). In line with the high Al content in the parent zeolite, the filtrate collected after treatment with 1.0 M NaOH evidenced a relatively low Si/Al ratio (89, Table 1).²⁰ The preferential removal of Si reduced the Si/Al ratio of the solid to 3 (1.0NaOH). Also 1.4NaOH, which displayed a similar weight loss upon alkaline treatment, comprised a Si/Al ratio of 3.

In agreement with the mesopore surface areas observed in (Figure 2c), increased uptakes at middle-to-high relative pressures showed for the treated Z15 samples 0.6NaOH and 1.0NaOH (Figure 1b,c). The external surface areas accounted to 147 m² g⁻¹ (0.6NaOH) and 236 m² g⁻¹ (1.0NaOH). On the other hand, reduced uptakes at lowest relative pressures relate to lower micropore volumes. For example, the micropore volume of 0.6NaOH dropped slightly to 0.13 cm³ g⁻¹, whereas for 1.0NaOH a $V_{\text{micro}} = 0.05 \text{ cm}^3 \text{ g}^{-1}$ was obtained. More pronounced reductions in micropore volume (down to 0.02 cm³ g⁻¹) were observed on treatment of Z10 (Table SII). For Z15, treatment at 1.4 M NaOH

1 resulted in a rather limited S_{meso} ($69 \text{ m}^2 \text{ g}^{-1}$), whereas V_{micro} was reduced to $0.11 \text{ cm}^3 \text{ g}^{-1}$.

2
3 The mesopore size distribution of sample 0.6NaOH revealed the presence of contributions centered
4 roughly near 3 nm and 35 nm (Inset in [Figure 1b](#)). More severe alkaline treatment led to the presence of
5 mesopores near 8 nm (1.0NaOH), while an absence of centered mesopores evidenced at even higher
6 concentration (1.4NaOH). Intracrystalline mesopores were clearly visible in the TEM micrographs of
7 0.6NaOH and 1.0NaOH ([Figure 4](#)). For sample 0.6NaOH, lattice fringes were evident throughout the
8 crystals and no evidence of zeolite amorphization was observed. More significant morphological
9 changes were observed for 1.0NaOH and 1.4NaOH, which should be related to the higher amount of Al-
10 rich debris present in these samples (*vide infra*). In agreement with the nitrogen adsorption, fewer intra-
11 crystalline mesopores are observed in 1.4NaOH.

12
13
14
15
16
17
18
19
20
21
22
23
24 [Figure 5](#) shows the development of S_{meso} , V_{micro} , and crystallinity with NaOH concentration in more
25 detail. Up to 1.0 M NaOH the obtained solids displayed a gradually increasing mesopore surface area up
26 to their maximum value, *i.e.* 100% or $236 \text{ m}^2 \text{ g}^{-1}$. Conversely, at higher concentrations (1.2-1.8 M) a
27 steep decrease down to *ca.* 30% was observed. The variation of microporosity displayed an almost
28 inverse relationship, decreasing down to *ca.* 35% at 1.0 M NaOH, then restoring to up to 80% at higher
29 molarities. Crystallinity displayed a similar trend, decreasing strongly up to 1.0 M NaOH (down to *ca.*
30 20%) after which it rose up to *ca.* 50% (selected XRD patterns are presented in [Figure SI2](#)). It seems
31 that two regimes of dissolution take place in the case of Z15, of which 1.0 M is the critical point. At
32 concentrations $< 1.0 \text{ M}$, a selective dissolution occurs resulting in the formation of mesopores and a
33 consequential reduction of crystallinity. At concentrations $> 1.0 \text{ M}$ the dissolution appears to be less
34 selective, resulting in a dissolution process similar to that of standard alkaline-treatment on silicalite-1.³⁰
35 Hence, the resulting samples display a low S_{meso} and a relatively high crystallinity.

36
37
38
39
40
41
42
43
44
45
46
47
48
49
50
51
52 The reduction of crystallinity upon the introduction of mesoporosity by desilication was thus far
53 mostly semi-quantitatively reported.^{12,14,18} [Figure 6](#) plots the crystallinities of alkaline-treated Z15 and
54 Z40 as a function of their corresponding mesopore surface areas. The resulting linear correlation
55
56
57
58
59
60

1 evidences that the crystallinity decreases with about 0.5% per $\text{m}^2 \text{g}^{-1}$ of external surface area for Z15,
2 which is roughly twice that of the crystallinity loss obtained after alkaline treatment of Z40 (ca. 0.25%
3 per $\text{m}^2 \text{g}^{-1}$). This discrepancy is further discussed in the next subsection.
4
5

6
7 ^{27}Al and ^{29}Si MAS NMR was performed to investigate the influence of the alkaline treatments on the
8 coordination of the Al and Si, respectively. As mentioned, ^{27}Al MAS NMR showed that the parent Z15
9 comprised mostly framework Al, as well as a minor amount of extra-framework Al. Upon alkaline
10 treatment the band attributed to framework Al (at 59 ppm) broadened whereas the minor contribution
11 related to extra-framework Al (at 0 ppm) was no longer distinguishable (Figure 7). We have recently
12 demonstrated that the band at 59 ppm can be attributed to both purely framework and (partially)
13 reintegrated Al.³⁰ It is therefore likely that, upon alkaline treatment, both the Al extracted from the
14 zeolite framework to form a mesopore, as well as the extra-framework aluminum, are partially
15 reintegrated in the framework. The broadening of the band at 59 ppm should consequently be due to the
16 co-presence of purely framework and (partially) reintegrated Al. Likely, the more pronounced
17 broadening of this band for 1.0NaOH compared to 1.4NaOH, should be due to a greater heterogeneity
18 of aluminum sites implied by the higher mesoporosity in the former sample. ^{29}Si MAS NMR performed
19 on both the parent and treated samples revealed the presence of mostly crystalline (Q_4) components with
20 chemical shifts centered around -112 ppm. Upon desilication, the components near -106 ppm increased,
21 reflecting the higher Al content in the zeolite (Figure SI3). However, no major amorphization, as for
22 example can occur upon desilication of FAU,¹⁷ was evidenced.
23
24
25
26
27
28
29
30
31
32
33
34
35
36
37
38
39
40
41
42
43
44

45 **Removal of Al-rich debris by acid treatment.** Previous work has shown that relatively mild acid
46 treatments can be used to selectively remove Al-rich debris from alkaline-treated zeolites.^{18,28,41} More
47 specifically, for ZSM-5 zeolites within the optimal Si/Al ratio (47) such treatment enabled restoration of
48 the Si/Al ratio to that of the parent zeolite and a significant reduction of the Lewis acidity, while
49 crystallinity and porosity remained mostly unaffected.²⁸ In the case of alkaline treatment of high-
50 alumina ZSM-5 (Si/Al < 20) a noticeable influence on crystallinity and porosity is more likely since the
51
52
53
54
55
56
57
58
59
60

1 amount of Al-rich debris is higher. We performed subsequent acid treatments to assess the influence of
2 the latter species.
3

4 **Table 2** presents 4 matrices in which the influence of an additional acid wash (0.02, 0.05, and 0.10 M
5 HCl) on the yield, crystallinity, V_{micro} , and S_{meso} is summarized. Acid treatments of the parent zeolite
6 resulted in high yields and little alteration of the porosity or crystallinity, attending to the high resistance
7 of the MFI structure in acid media.⁴² Conversely, the washing of the alkaline-treated zeolites resulted in
8 a greater modification of their properties. The yields decreased with increasing severity of the acid
9 treatment and the preceding alkaline treatment. This is unsurprising, since the amount of Al-rich debris
10 typically increase with the severity of the alkaline treatment.^{14,35} For example, sample 0.6NaOH (75%
11 yield) showed a 9% weight loss upon treatment with 0.10 M HCl (0.6NaOH-0.10HCl, 68% yield). On
12 the other hand, going from 1.0NaOH (39% yield) to 1.0NaOH-0.10HCl (28% yield) a drop of 28% was
13 observed. Elemental analysis revealed that sample 1.0NaOH-0.10HCl exhibits a Si/Al ratio similar (15)
14 to the parent zeolite (**Table 1**), which implies the removal of predominately Al-rich species. ²⁹Si MAS
15 NMR confirmed the removal of Al-rich species, evidencing a substantially increased similarity between
16 the sequentially-treated sample and the parent zeolite (**Figure SI3**).
17
18
19
20
21
22
23
24
25
26
27
28
29
30
31
32
33
34
35

36 Upon acid washing, the crystallinity increased substantially (**Table 2**). In fact, **Figure 6** shows a
37 significantly different linear due to the increase in both crystallinity and mesoporosity (*vide infra*). The
38 corresponding slope is halved to -0.25% per $\text{m}^2 \text{g}^{-1}$, and is now similar to the crystallinity loss for
39 alkaline-treated Z40. This clearly illustrates that upon alkaline treatment of low Si/Al ratio zeolites, the
40 loss of crystallinity should be ascribed to (i) the introduction of mesopores, and (ii) the presence of
41 amorphous Al-rich debris.
42
43
44
45
46
47
48
49

50 The N_2 isotherms derived from the alkaline and acid-treated samples revealed the detrimental
51 influence of the formed Al-rich debris on the porous properties. **Figures 1b,c** show increased uptakes at
52 both low and middle-to-high relative pressures, which is reflected in gradual increases in V_{micro} and
53 S_{meso} , respectively (**Table 2**). Sample 0.6NaOH-0.10HCl evidenced an external mesopore surface area
54
55
56
57
58
59
60

1 that increased from $147 \text{ m}^2 \text{ g}^{-1}$ (0.6NaOH) to $173 \text{ m}^2 \text{ g}^{-1}$, whereas V_{micro} increased from $0.13 \text{ cm}^3 \text{ g}^{-1}$
2 (0.6NaOH) to $0.16 \text{ cm}^3 \text{ g}^{-1}$. Even more significant was the change for 1.0NaOH: S_{meso} rose from
3 $236 \text{ m}^2 \text{ g}^{-1}$ (1.0NaOH) to $341 \text{ m}^2 \text{ g}^{-1}$ (1.0NaOH-0.10HCl), and V_{micro} increased from $0.05 \text{ cm}^3 \text{ g}^{-1}$
4 (1.0NaOH) to $0.14 \text{ cm}^3 \text{ g}^{-1}$ (1.0NaOH-0.10HCl). Similar trends were observed upon acid treatment of
5 alkaline-treated Z10 (to yield 1.2NaOH-0.10HCl, Figure 1a). In the latter case, an increase of the
6 external surface (from $163 \text{ m}^2 \text{ g}^{-1}$ to $275 \text{ m}^2 \text{ g}^{-1}$) proved that alkaline treatment is also effective for MFI
7 zeolites comprising very low Si/Al ratios. Moreover, this implies that the presence of substantial extra-
8 framework aluminum in the parent zeolite does not inhibit the introduction of mesoporosity by
9 desilication.

10 Inspection of the BJH mesopore size distribution associated with the treated Z15 zeolites confirmed
11 that the mesoporosity of 0.6NaOH-0.10HCl remained mostly unaffected. On the other hand, for
12 1.0NaOH-0.10HCl, the intensity of the contributions around 8 nm increased substantially, attending to
13 the large increase in mesoporosity. TEM shows that zeolites treated at 0.6 M NaOH did not display
14 significant differences before and after HCl washing. Conversely, for zeolite 1.0NaOH-0.1HCl the
15 crystallites appeared more transparent to the electron beam, with sharper edge definition (Figure 4). This
16 indicates that the Al-rich debris are only noticeable (by TEM) at high relative abundance.

17 With the substantial increase of V_{micro} and S_{meso} , and the reduced yield after acid treatment, our
18 analyses using descriptors required refinement. For example, the indexed hierarchy factor increased
19 from 0.30 (0.6NaOH) and 0.18 (1.0NaOH), to 0.43 (0.6NaOH-0.10HCl) and 0.74 (1.0NaOH-0.10HCl),
20 respectively (Table SII). The latter exceeding the highest value obtained for alkaline-treated Z40
21 (IHF = 0.69). The positive influence on the desilication efficiency was less obvious since, although S_{meso}
22 increased, yields decreased. For Z15, when the increased external surface areas and the lower yields
23 were taken into account (after 0.10 M HCl treatment, Table 2), it proved that the desilication efficiency
24 increased by one-third (*ca.* $1 \text{ m}^2 \text{ g}^{-1} \%^{-1}$) to over $4 \text{ m}^2 \text{ g}^{-1} \%^{-1}$. In the case of Z10, the desilication
25 efficiency doubled to $2 \text{ m}^2 \text{ g}^{-1} \%^{-1}$. As mentioned previously, the introduction of large degrees of S_{meso} in
26
27
28
29
30
31
32
33
34
35
36
37
38
39
40
41
42
43
44
45
46
47
48
49
50
51
52
53
54
55
56
57
58
59
60

1 silicalite-1 was achieved by including external pore-direction agents (*e.g.* AlO_4^-) in the alkaline
2 solution.³⁰ The resulting hierarchical silicalite-1 (Z1000 in Figure 3) comprised a similar porosity
3 compared to alkaline-treated ZSM-5 with Si/Al ratio within the optimal range ($S_{\text{meso}} > 200 \text{ m}^2 \text{ g}^{-1}$).
4 Moreover, the yield increased, implying concomitantly a comparable desilication efficiency of *ca.*
5 $5 \text{ m}^2 \text{ g}^{-1} \%^{-1}$. Consequently, as is illustrated in Figure 3b, the efficiency of desilication can be increased
6 by either sequential alkaline-acid treatment (in the case of Al-rich zeolites) or by the use of external
7 PDA (in the case of all-silica zeolites).
8

9
10
11
12
13
14
15
16
17 ***Acid properties and catalytic evaluation.*** To investigate the functionality of the parent and
18 hierarchical zeolites we have examined the acidity and catalytic performance of selected Al-rich (Z15)
19 samples. The acidity of the parent and treated zeolites was studied by NH_3 -TPD and infrared
20 spectroscopy in the OH stretching region. Figure 8a reveals 3 principal absorbance bands in the IR
21 spectrum of the parent zeolite. The most intense band, present around 3600 cm^{-1} , relates to the Brønsted
22 acid sites. The band at 3740 cm^{-1} , which arises from isolated terminal silanols, displayed a substantial
23 intensity due to the considerable external surface present in the parent sample. The weaker band at
24 3650 cm^{-1} could be related to extra- or partial framework aluminum,¹⁹ consistent with ^{27}Al MAS NMR.
25 Figure 8b shows the NH_3 -TPD profiles of the parent and treated zeolites. Sample P comprised mostly
26 strong acid sites, showing the typical desorption peak around 750 K. Additionally, a shoulder around
27 570 K is evidenced which should be attributed to Lewis acidity related to extra-framework aluminum.¹⁹
28
29
30
31
32
33
34
35

36
37
38
39
40
41
42
43 Upon alkaline treatment, the band at 3740 cm^{-1} in the IR spectrum of sample 0.6NaOH increased,
44 attending to the higher external surface. However, the intensity was not as pronounced as previously
45 reported for mesoporous Z40 prepared by desilication.¹⁹ In addition, the band at 3600 cm^{-1} , related to
46 Brønsted acid sites, was no longer clearly distinguishable: instead a broad band around 3570 cm^{-1}
47 presented. Contributions in this region are typically associated with hydrogen bonding between
48 neighboring hydroxyl groups, *e.g.* at defect sites, within the zeolite structure. These likely originate
49 from the deposited Al-rich debris.^{18,41} The contribution at 3650 cm^{-1} , although slightly broadened,
50
51
52
53
54
55
56
57
58
59
60

1 remained present. As no evidence of octahedrally-coordinated Al was observed in the alkaline-treated
2 zeolites by ^{27}Al MAS NMR, this demonstrates that the band at 3650 cm^{-1} can arise from hydroxyls
3 associated with tetrahedral (*e.g.* partially coordinated) Al species. The NH_3 -TPD profile of the alkaline-
4 treated sample 0.6NaOH displayed a similar contribution around 750 K compared to the parent, which
5 proves that, unlike is suggested by the IR spectrum of 0.6NaOH, the strong (Brønsted) acidity was
6 preserved. In addition, a more pronounced shoulder can be observed around 570 K, attending to the
7 increase in Lewis acidity due to the Al-rich deposits.³⁰ Quantification of the total acidity by integration
8 shows that 0.6NaOH comprises a total acidity 1.3 times higher than that of the parent zeolite.
9

10 Upon subsequent acid washing (sample 0.6NaOH-0.02HCl), the intensity of the band at 3740 cm^{-1}
11 increased, the contribution related to Brønsted acid sites at 3600 cm^{-1} largely restored, and the broad
12 band at 3570 cm^{-1} was no longer discernable. It is therefore likely that the Al-debris in 0.6NaOH
13 masked some of the contributions in OH stretching region of the infrared spectrum. The NH_3 -TPD
14 profile evidenced that the contribution around 570 K was significantly lower whereas the peak related to
15 the intrinsic Brønsted acidity (at 750 K) was mostly preserved. The removal of Al from the sample is
16 corroborated by the reduction of the total acidity from 1.3 to approximately 1.1 times that of the parent
17 zeolite. These results, combined with those from elemental analysis, confirm the restoration of the acid
18 properties upon removal of the Al-rich debris by the acid washing step.
19

20 The catalytic activity of P, 0.6NaOH, and 0.6NaOH-0.02HCl zeolites was examined in the alkylation
21 of toluene with benzyl alcohol (Figure 9). The alkaline-treated sample (0.6NaOH) displayed a
22 conversion of benzyl alcohol (X_{BA}) around 3 times higher compared to the parent zeolite (averaging
23 X_{BA} 's at $t = 5$ and $t = 10$ min). The improved performance should be related to the introduced
24 mesoporosity, increasing the accessibility of, and transport to, the active sites located in the micropores.
25 The subsequent acid wash proved of great importance, enhancing the catalytic activity to over 5 times
26 that of the parent, hereby evidencing a suppressing influence of the Al-rich debris on the activity. The
27 inset in Figure 9 shows that the conversion of benzyl alcohol relates linearly to the IHFs. In the case of
28
29
30
31
32
33
34
35
36
37
38
39
40
41
42
43
44
45
46
47
48
49
50
51
52
53
54
55
56
57
58
59
60

1 benzene alkylation with ethylene,²⁶ a similar trend was observed between the ethylbenzene productivity
2 and the hierarchy factor of mesoporous Z40 prepared by desilication. Our results confirm the strong
3 dependency of the alkylation performance on both meso- and microporosity, and stress the strength of
4 the (indexed) hierarchy factor.
5
6
7
8

9
10 Clearly, in the preparation of the mesoporous low Si/Al ratio zeolites by desilication it is essential to
11 remove Al-rich debris by a sequential alkaline treatment. Similarly, it also proved that upon introduction
12 of mesoporosity in unidirectional ZSM-22 zeolites (Si/Al = 42) by alkaline treatment the removal of
13 these Al-rich species by a subsequent acid washing is highly beneficial.¹⁸ Figure 10 schematically
14 illustrates why, especially for zeolite crystals comprising a limited micropore dimensionality and/or a
15 high Al content, the sequential acid treatment is of such paramount importance. Scenario (1a-c)
16 represents unidirectional microporous crystals of optimal Si/Al ratio (after ref. 18), whereas scenario
17 (2a-c) represents 2D or 3D crystals that contain significantly more aluminum (after this work). In both
18 scenarios the alkaline treatment leads to the introduction of mesoporosity. However the accessibility to
19 the micropore volume is not optimal due to the deposition of Al-rich debris, blocking part of the
20 micropore mouths. In the case of 1b this is implied by the high tendency of the unidirectional crystal to
21 be blocked, whereas in 2b this is caused by the high Al content. In both cases, a subsequent acid wash
22 (1c, 2c) is essential to remove the Al-rich debris and unblock the micropore mouths, hereby further
23 increasing accessibility and restoring the micropore volume.
24
25
26
27
28
29
30
31
32
33
34
35
36
37
38
39
40
41
42
43
44

45 **4. Conclusions**

46
47 Full compositional flexibility in the preparation of mesoporous MFI zeolites by desilication was
48 achieved. A systematic 2-dimensional screening, as a function of the Si/Al ratio in the parent material
49 and NaOH concentration, enabled assessment of the entire spectrum of solids than can be obtained by
50 alkaline treatment. Desilication by NaOH alone proved effective in the Si/Al range of 12-200, and most
51 efficient in the previously established range 25-50. The operational window of alkaline treatment is
52
53
54
55
56
57
58
59
60

1 limited by the Al content of the parent zeolite: the absence of aluminum leads to the formation of mostly
2 macropores, and an excess of aluminum results in blockage of micro- and mesopores by the formation
3 of amorphous Al-rich deposits. Effective mesopore formation in these extremes can be attained by
4 of amorphous Al-rich deposits. Effective mesopore formation in these extremes can be attained by
5 either the addition of external pore-directing agent to the alkaline solution (all-silica zeolites) or the use
6 of a sequential acid wash (Al-rich zeolites). The latter acid treatment not only leads to the uncovering of
7 the full porosity; it also increases crystallinity and restores the Si/Al ratio and acidity. Catalytic
8 evaluation of selected zeolites in the toluene alkylation with benzyl alcohol confirmed the superiority of
9 the alkaline-treated (mesoporous) sample to the purely microporous material. This is attributed to the
10 improved access of, and transport to, the active sites located in the zeolite micropores. Moreover, the
11 acid washing step after desilication demonstrated essential, further enhancing the activity of the
12 hierarchical zeolite. The desilication efficiency proved a powerful descriptor to evaluate the gain in
13 mesoporosity with respect to the weight loss upon application of the post-synthesis treatments. The
14 (indexed) hierarchy factor was highly useful in categorizing the obtained hierarchical structures and
15 relating them to catalytic performance.

16
17
18
19
20
21
22
23
24
25
26
27
28
29
30
31
32
33
34
35
36 **Acknowledgement.** ETH Zürich is acknowledged for financial support.

37
38
39
40 **Supporting Information Available.** Summary of characterization, additional MAS NMR spectra, and
41 XRD patterns. This material is available free of charge via the Internet at <http://pubs.acs.org>.
42
43
44
45
46

47 **References**

- 48
49
50 (1) Pérez-Ramírez, J.; Christensen, C. H.; Egeblad, K.; Christensen, C. H.; Groen, J. C. *Chem. Soc.*
51 *Rev.* **2008**, *37*, 2530.
52
53
54 (2) Schmidt, W. *ChemCatChem* **2009**, *1*, 53.
55
56
57 (3) Chal, R.; Gérardin, C.; Bulut, M.; van Donk, S. *ChemCatChem* **2011**, *3*, 67.
58
59
60

- 1 (4) Egeblad, K.; Christensen, C. H.; Kustova, M. Yu.; Christensen, C. H. *Chem. Mater.* **2008**, *20*, 946.
2
3 (5) Groen, J. C.; Peffer, L. A. A.; Moulijn, J. A.; Pérez-Ramírez, J. *J. Mater. Chem.* **2006**, *16*, 2121.
4
5 (6) Groen, J. C.; Moulijn, J. A.; Pérez-Ramírez, J. *Ind. Eng. Chem. Res.* **2007**, *46*, 4193.
6
7 (7) Groen, J. C.; Peffer, L. A. A.; Moulijn, J. A.; Pérez-Ramírez, J. *Microporous Mesoporous Mater.*
8
9 **2004**, *69*, 29.
10
11 (8) Wei, X.; Smirniotis, P. G. *Microporous Mesoporous Mater.* **2006**, *97*, 97.
12
13 (9) Groen, J. C.; Sano, T.; Moulijn, J. A.; Pérez-Ramírez, J. *J. Catal.* **2007**, *251*, 21.
14
15 (10) Groen, J. C.; Abelló, S.; Villaescusa, L. A.; Pérez-Ramírez, J. *Microporous Mesoporous Mater.*
16
17 **2008**, *114*, 93.
18
19 (11) Pérez-Ramírez, J.; Abelló, S.; Villaescusa, L. A.; Bonilla, A. *Angew. Chem. Int. Ed.* **2008**, *47*,
20
21 7913.
22
23 (12) Bonilla, A.; Baudouin, D.; Pérez-Ramírez, J. *J. Catal.* **2009**, *265*, 170.
24
25 (13) Mokrzycki, Ł.; Sulikowski, B.; Olejniczak, Z. *Catal. Lett.* **2009**, *127*, 296.
26
27 (14) Verboekend, D.; Groen, J. C.; Pérez-Ramírez, J. *Adv. Funct. Mater.* **2010**, *20*, 1441.
28
29 (15) Musilová-Pavlačková, Z.; Zones, S. I.; Čejka, J. *Top. Catal.* **2010**, *53*, 273.
30
31 (16) Sommer, L.; Mores, D.; Svelle, S.; Stöcker, M.; Weckhuysen, B. M.; Olsbye, U. *Microporous*
32
33 *Mesoporous Mater.* **2010**, *132*, 384.
34
35 (17) de Jong, K. P.; Zečević, J.; Friedrich, H.; de Jongh, P. E.; Bulut, M.; van Donk, S.; Kenmogne, R.;
36
37 Finiels, A.; Hulea V.; Fajula, F. *Angew. Chem., Int. Ed.* **2010**, *49*, 10074.
38
39 (18) Verboekend, D.; Chabaneix, A. M.; Thomas, K.; Gilson, J.-P.; Pérez-Ramírez, J. *CrystEngComm*
40
41 **2011**, *13*, 3408.
42
43 (19) Groen, J. C.; Jansen, J. C.; Moulijn, J. A.; Pérez-Ramírez, J. *J. Phys. Chem. B* **2004**, *108*, 13062.
44
45 (20) Groen, J. C.; Peffer, L. A. A.; Moulijn, J. A.; Pérez-Ramírez, J. *Chem. Eur. J.* **2005**, *11*, 4983.
46
47 (21) Groen, J. C.; Caicedo-Realpe, R.; Abelló, S.; Pérez-Ramírez, J. *Mater. Lett.* **2009**, *63*, 1037.
48
49 (22) Pérez-Ramírez, J.; Abelló, S.; Bonilla, A.; Groen, J. C. *Adv. Funct. Mater.* **2009**, *19*, 164.
50
51
52
53
54
55
56
57
58
59
60

- 1
2
3
4
5
6
7
8
9
10
11
12
13
14
15
16
17
18
19
20
21
22
23
24
25
26
27
28
29
30
31
32
33
34
35
36
37
38
39
40
41
42
43
44
45
46
47
48
49
50
51
52
53
54
55
56
57
58
59
60
- (23) Abelló, S.; Pérez-Ramírez, J. *Phys. Chem. Chem. Phys.* **2009**, *11*, 2959.
- (24) Abelló, S.; Bonilla, A.; Pérez-Ramírez, J. *Appl. Catal. A* **2009**, *364*, 191.
- (25) Caicedo-Realpe, R.; Pérez-Ramírez, J. *Microporous Mesoporous Mater.* **2010**, *128*, 91.
- (26) Pérez-Ramírez, J.; Verboekend, D.; Bonilla, A.; Abelló, S. *Adv. Funct. Mater.* **2009**, *19*, 3972.
- (27) Groen, J. C.; Moulijn, J. A.; Pérez-Ramírez, J. *Microporous Mesoporous Mater.* **2005**, *87*, 153.
- (28) Fernandez, C.; Stan, I.; Gilson, J.-P.; Thomas, K.; Vicente, A.; Bonilla, A.; Pérez-Ramírez, J. *Chem. Eur. J.* **2010**, *16*, 6224.
- (29) Thibault-Starzyk, F.; Stan, I.; Abelló, S.; Bonilla, A.; Thomas, K.; Fernandez, C.; Gilson, J.-P.; Pérez-Ramírez, J. *J. Catal.* **2009**, *264*, 11.
- (30) Verboekend, D.; Pérez-Ramírez, J. *Chem. Eur. J.* **2011**, *17*, 1137.
- (31) Kustova, M. Yu.; Kustov, A. L.; Christensen, C. H. *Stud. Surf. Sci. Catal.* **2005**, *158*, 255.
- (32) van Laak, A. N. C.; Safala, S. L.; Zečević, J.; Friedrich, H.; de Jongh, P. E.; de Jong, K. P. *J. Catal.* **2010**, *276*, 170.
- (33) Gil, B.; Mokrzycki, Ł.; Sulikowski, B.; Olejniczak, Z.; Walas, S. *Catal. Today* **2010**, *152*, 24.
- (34) Zhao, L.; Xu, C.; Gao, S. *J. Mater. Sci.* **2010**, *45*, 5406.
- (35) van Miltenburg, A.; Pawlesa, J.; Bouzga, A. M.; Žilkova, N.; Čejka, J.; Stöcker, M. *Top Catal.* **2009**, *52*, 1190.
- (36) Paixao, V.; Carvalho, A. P.; Rocha, J.; Fernandes, A.; Martins, A. *Microporous Mesoporous Mater.* **2010**, *131*, 350.
- (37) Lippens, B. C.; de Boer, J. H. *J. Catal.* **1965**, *4*, 319.
- (38) Brunauer, S.; Emmett, P. H.; Teller, E. *J. Am. Chem. Soc.* **1938**, *60*, 309.
- (39) Barrett, E. P.; Joyner, L. G.; Halenda, P. P. *J. Am. Chem. Soc.* **1951**, *73*, 373.
- (40) Čížmek, A.; Subotić, B.; Šmit, I.; Tonejc, A.; Aiello, R.; Crea, F.; Nastro, A. *Microporous Mater.* **1997**, *8*, 159.
- (41) Verboekend, D.; Caicedo-Realpe, R.; Bonilla, A.; Santiago, M.; Pérez-Ramírez, J. *Chem. Mater.*

1 **2010**, 22, 4679.

2
3 (42) Oumi, Y.; Nemoto, S.; Nawata, S.; Fukushima, T.; Teranishi, T.; Sano, T. *Mater. Chem. Phys.*

4
5 **2002**, 78, 551.

6
7
8
9
10
11
12
13
14
15
16
17
18
19
20
21
22
23
24
25
26
27
28
29
30
31
32
33
34
35
36
37
38
39
40
41
42
43
44
45
46
47
48
49
50
51
52
53
54
55
56
57
58
59
60

Tables

Table 1. Chemical composition of selected zeolites and filtrates obtained by alkaline and acid treatments of Z15.

Sample	Si/Al ^a (mol mol ⁻¹)	Si/Al _{filtrate} ^a (mol mol ⁻¹)
P	15	-
1.0NaOH	3	89
1.4NaOH	3	-
1.0NaOH-0.1HCl	15	-

^a Atomic absorption spectroscopy.

Table 2. Yield, crystallinity, and porosity of alkaline and acid-treated Z15 zeolites.

	Yield (%)			Crystallinity (%)			HCl (M)			V_{micro} ($\text{cm}^3 \text{g}^{-1}$)	S_{meso} ($\text{m}^2 \text{g}^{-1}$)					
	0	0.02	0.05	0.1	0	0.02	0.05	0.1	0			0.02	0.05	0.1		
NaOH (M)	0	0.02	0.05	0.1	0	0.02	0.05	0.1	0	0.02	0.05	0.1				
0	100	99	100	100	100	96	97	98	0.14	0.15	0.16	0.16	76	70	58	56
0.6	75	75	74	68	53	60	61	68	0.13	0.15	0.16	0.16	147	158	160	173
0.8	52	51	47	43	26	30	44	43	0.12	0.14	0.14	0.15	228	273	299	301
1.0	39	38	34	28	18	24	24	26	0.05	0.08	0.11	0.14	236	240	288	341
1.4	37	-	-	27	41	-	-	56	0.11	-	-	0.14	69	-	-	137

Figure captions

Figure 1. N₂ isotherms of parent and treated Z10 (a), Z15 (b,c) Z40 (d), Z1000 (e) zeolites. The insets represent the BJH mesopore size distributions.

Figure 2. Contour plots obtained by two-dimensional screening of alkaline treatments performed on MFI zeolites, as a function of the bulk Si/Al ratio of the parent zeolites (y-axis) and concentration NaOH (x-axis). The influence of the zeolite type and treatment condition on the yield (a), crystallinity (b), S_{meso} (c), V_{micro} (d), S_{BET} (e), V_{pore} (f), indexed hierarchy factor (IHF) (g), and IHF times yield (h) is shown.

Figure 3. Linear relationship between the increase in introduced mesopore surface area ($\Delta S_{\text{meso}} = S_{\text{meso,AT}} - S_{\text{meso,P}}$) and the weight loss upon desilication of ZSM-5 zeolites with framework Si/Al ratios in the range 10-1000 (a). The slopes of the linear trends represent the desilication efficiency ($\text{m}^2 \text{g}^{-1} \%^{-1}$). Variation in desilication efficiency with respect to the Si/Al ratio of the parent zeolite (b). The desilication efficiency of conventional alkaline treatment (solid symbols) is optimal for zeolites with Si/Al ratio = 25-50. Open symbols indicate the increased desilication efficiency due to either subsequent acid washing (HCl) for Al-rich zeolites (this work), or the use of external pore-directing agents (AlO_4^-) in the case of all-silica zeolites.³⁰

Figure 4. TEM images of parent and treated Z15 zeolites. The same scale bar applies to all the micrographs.

Figure 5. Influence of NaOH concentration on yield and crystallinity (a), and on micro- and mesoporosity (b) of alkaline-treated Z15. The parent zeolite is represented at 0 M.

1 **Figure 6.** Influence of mesoporosity on crystallinity of treated Z15 (triangles) and Z40 (circles) zeolites.
2
3 The solid symbols represent alkaline-treated samples (NaOH concentrations < 1 M), and the open
4
5 triangles represented the influence of a sequential acid treatment (0.1 M HCl).
6
7
8

9 **Figure 7.** ^{27}Al MAS NMR of parent and alkaline treated Z15 zeolites. The asterisk marks a spinning
10
11 side band.
12
13

14 **Figure 8.** Infrared spectra in the OH stretching region (a) and NH_3 -TPD profiles (b) of parent and
15
16 treated Z15 zeolites.
17
18
19

20 **Figure 9.** Conversion of benzyl alcohol (BA) over parent and treated Z15 zeolites in alkylation of
21
22 toluene (T) with benzyl alcohol. Conditions: $T/\text{BA} = 80$, $T = 433$ K, and $P = 0.5$ MPa. The inset relates
23
24 the conversion of benzyl alcohol at $t = 10$ min to the indexed hierarchy factor of each zeolite.
25
26
27
28
29

30 **Figure 10.** Schematic representation of the influence of the dimensionality and Si/Al ratio on the
31
32 micropore blockage by Al-rich debris on the external surface upon sequential alkaline and acid
33
34 treatment.
35
36
37
38
39
40
41
42
43
44
45
46
47
48
49
50
51
52
53
54
55
56
57
58
59
60

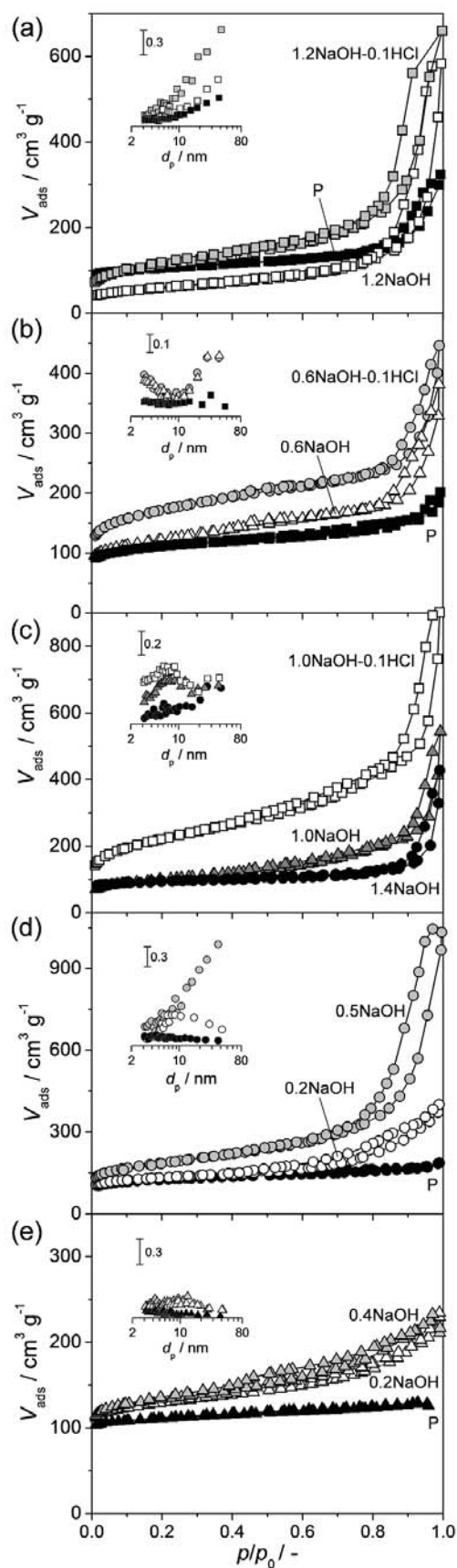


Figure 1

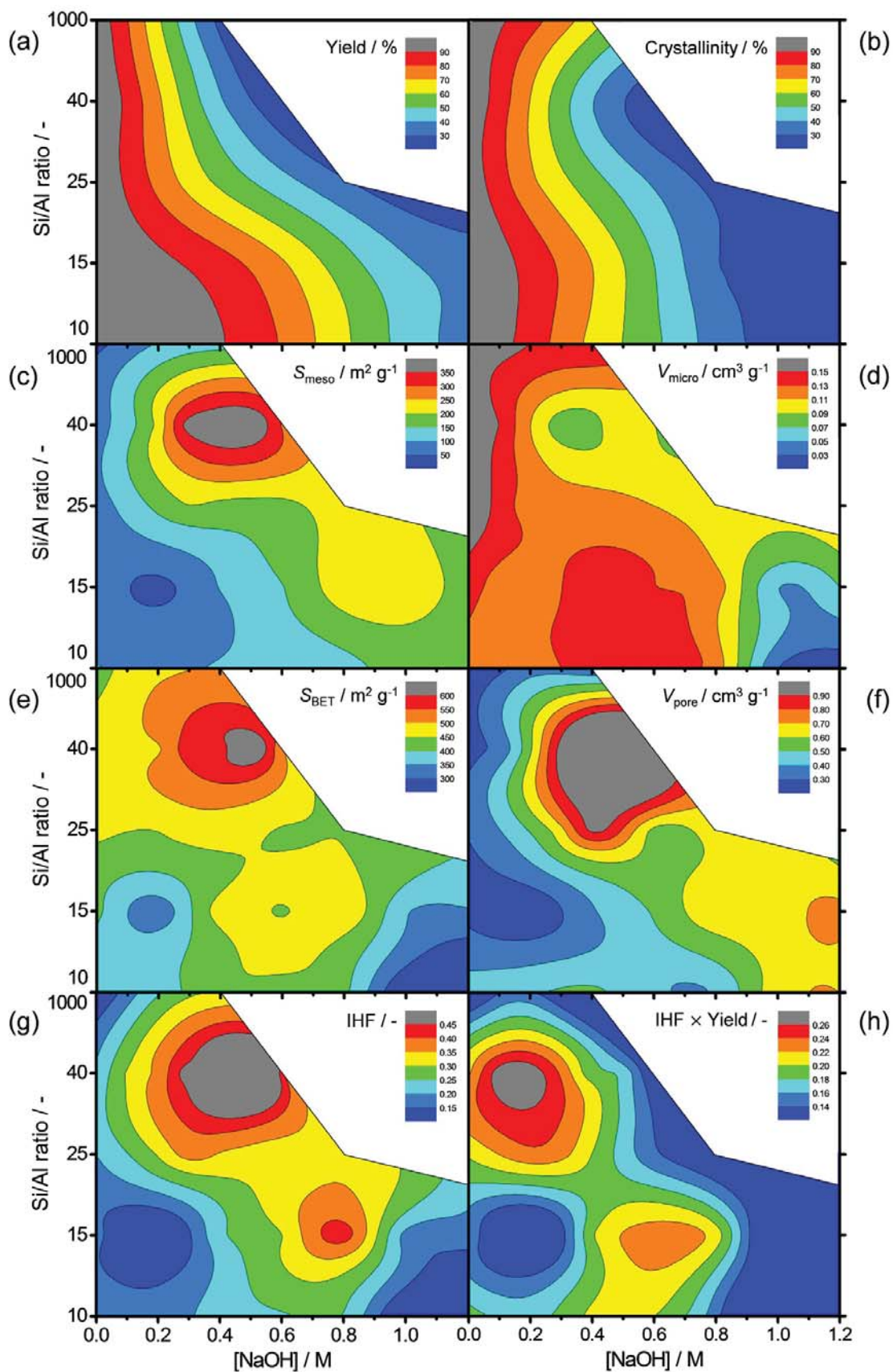


Figure 2

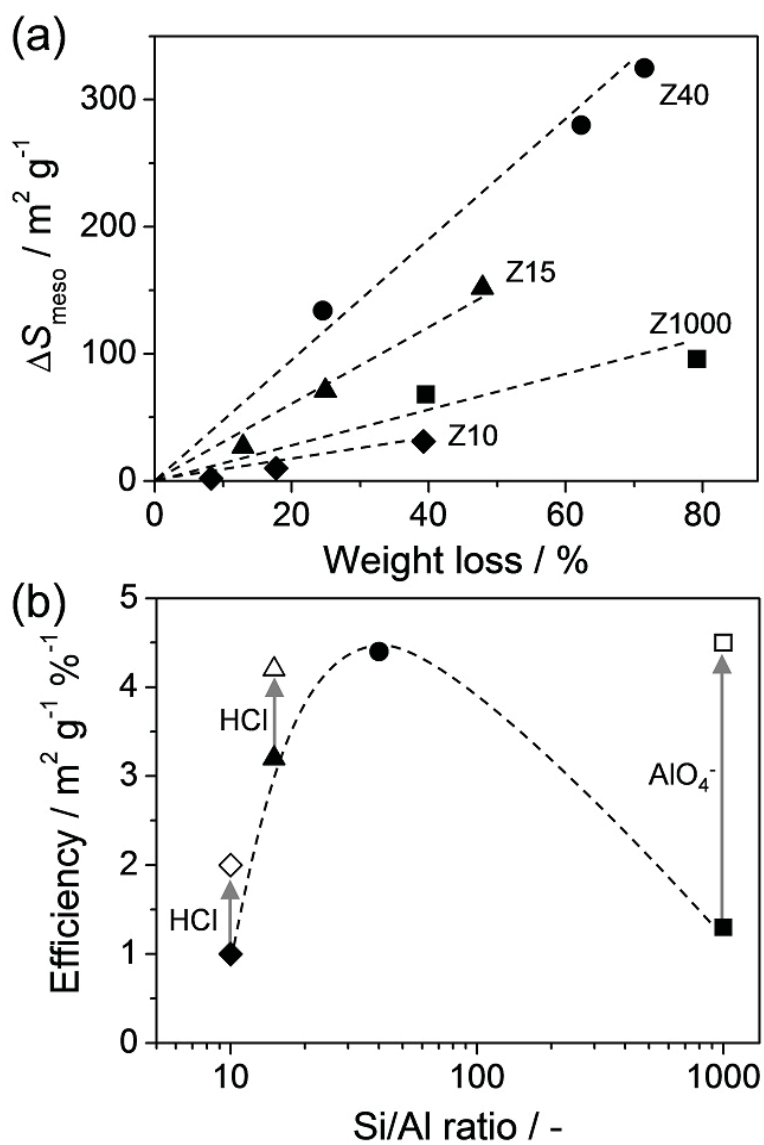


Figure 3

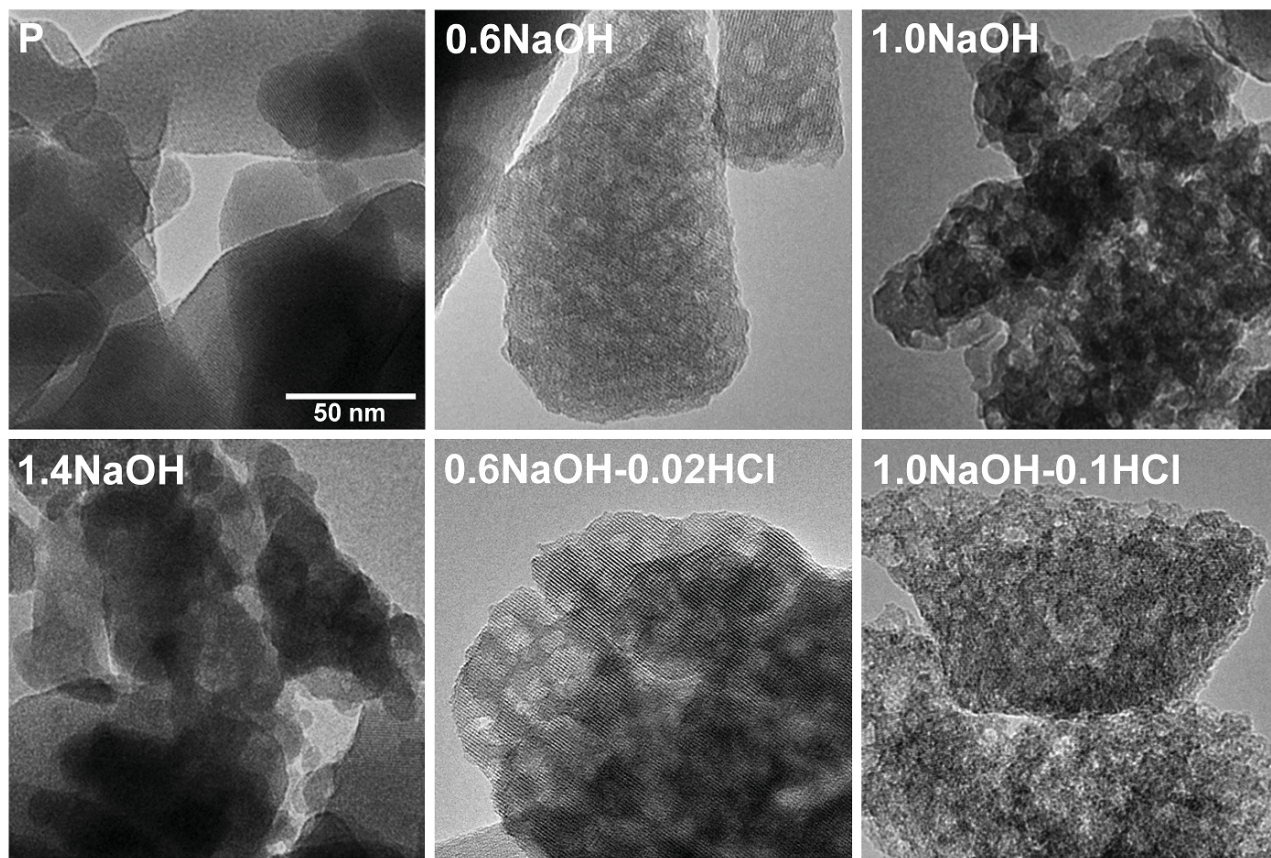


Figure 4

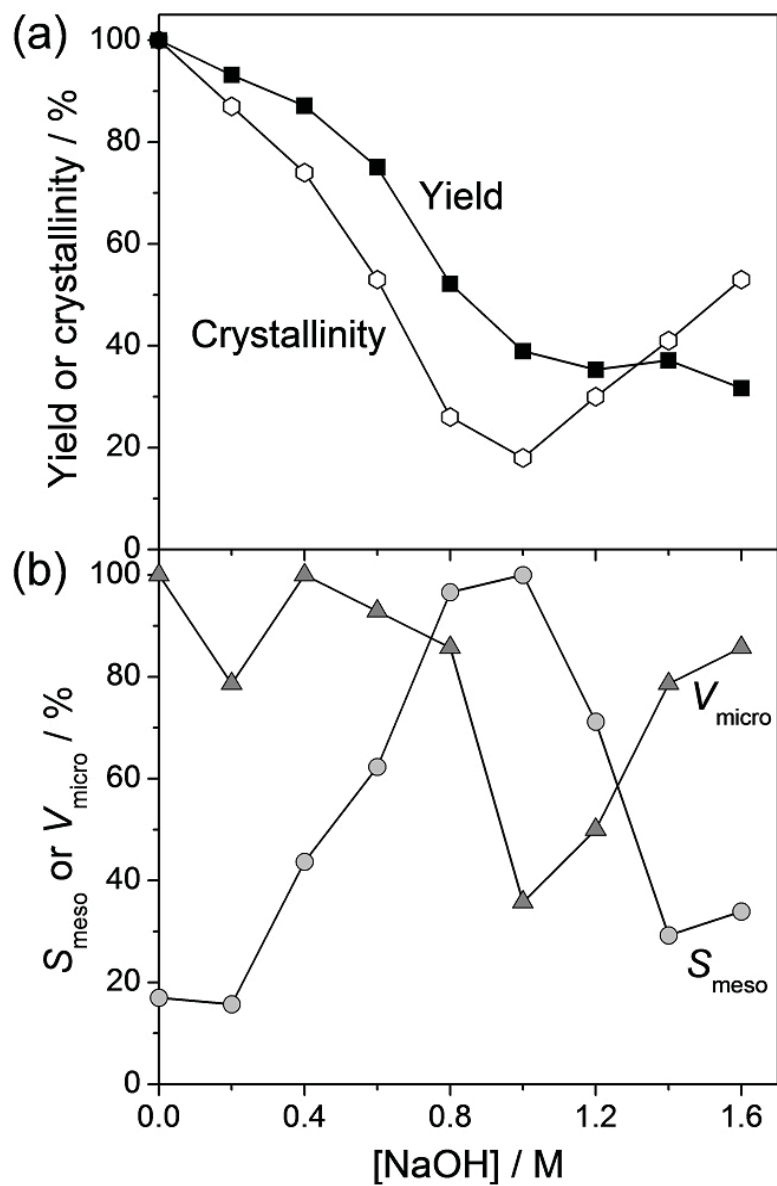


Figure 5

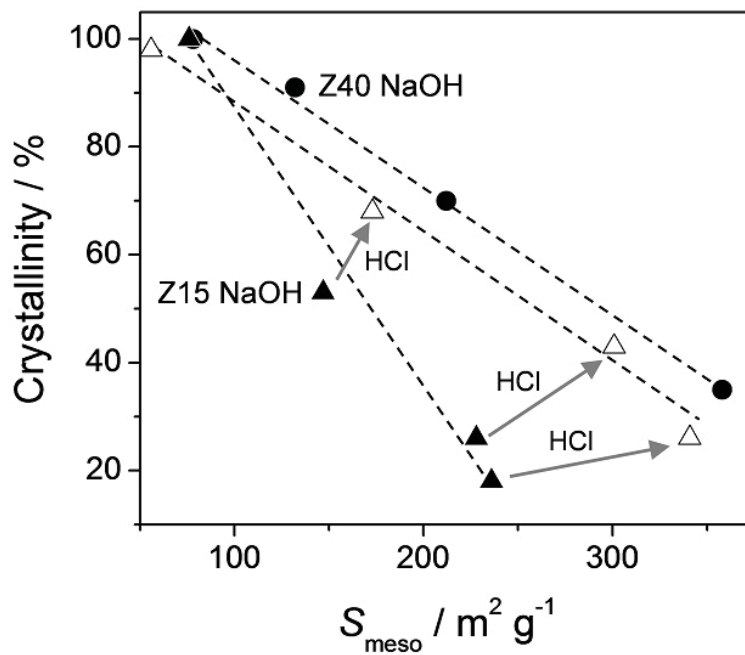


Figure 6

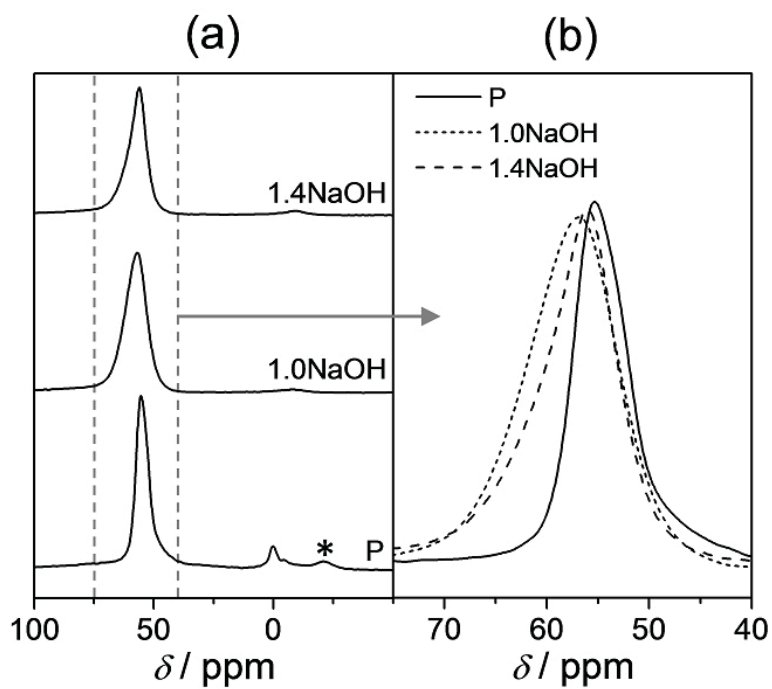


Figure 7

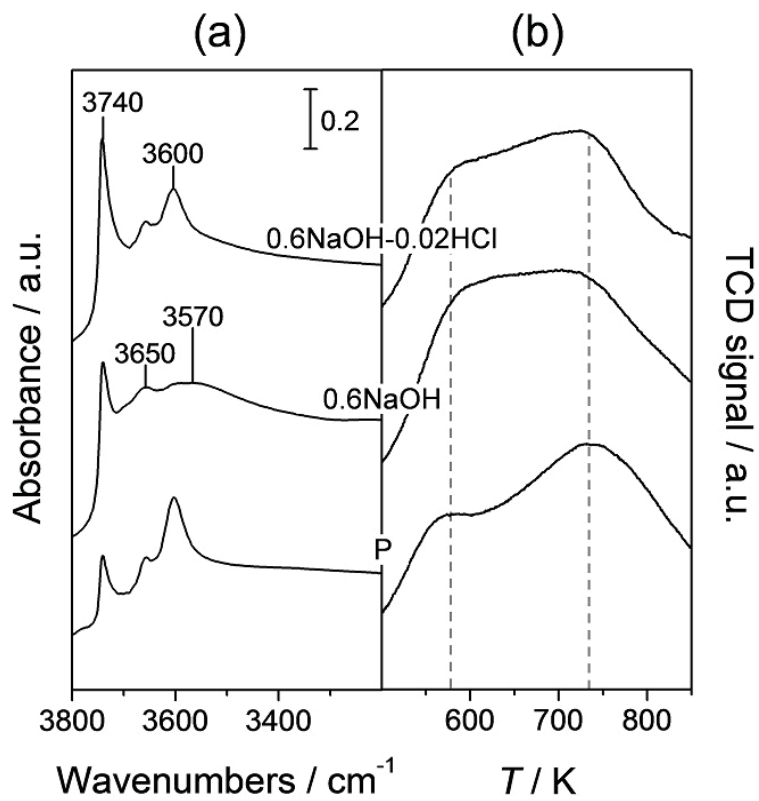


Figure 8

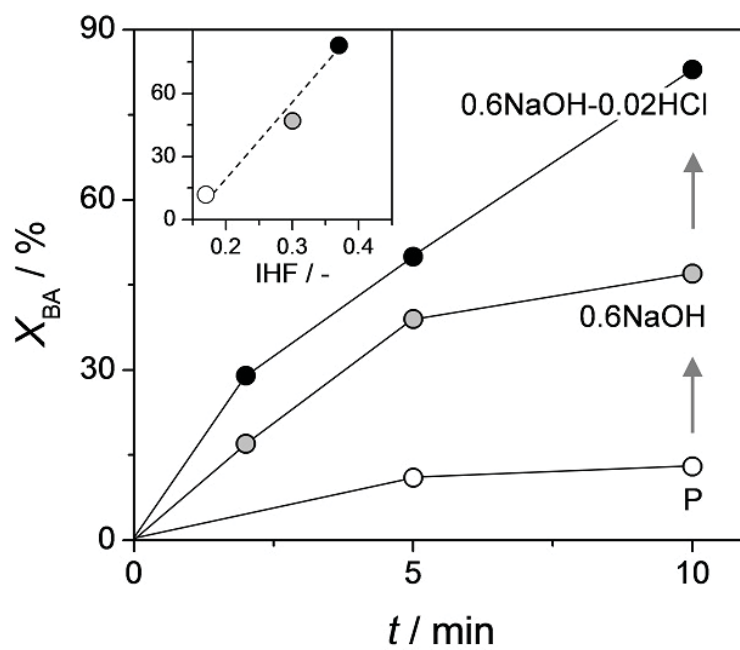


Figure 9

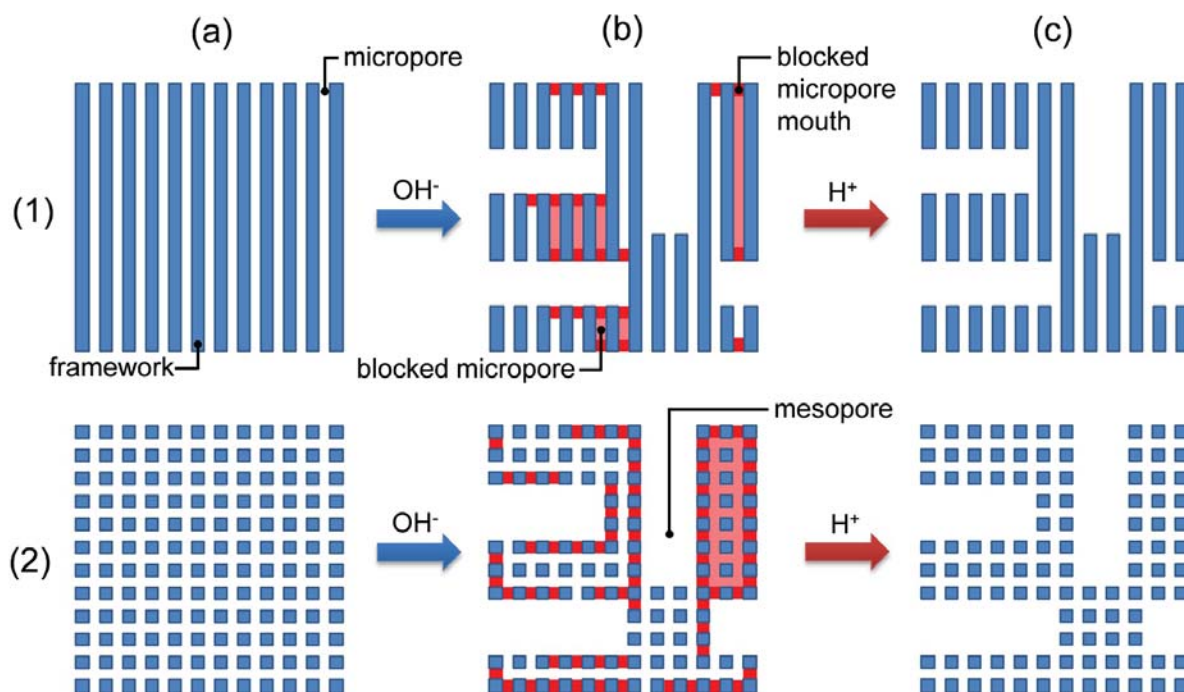
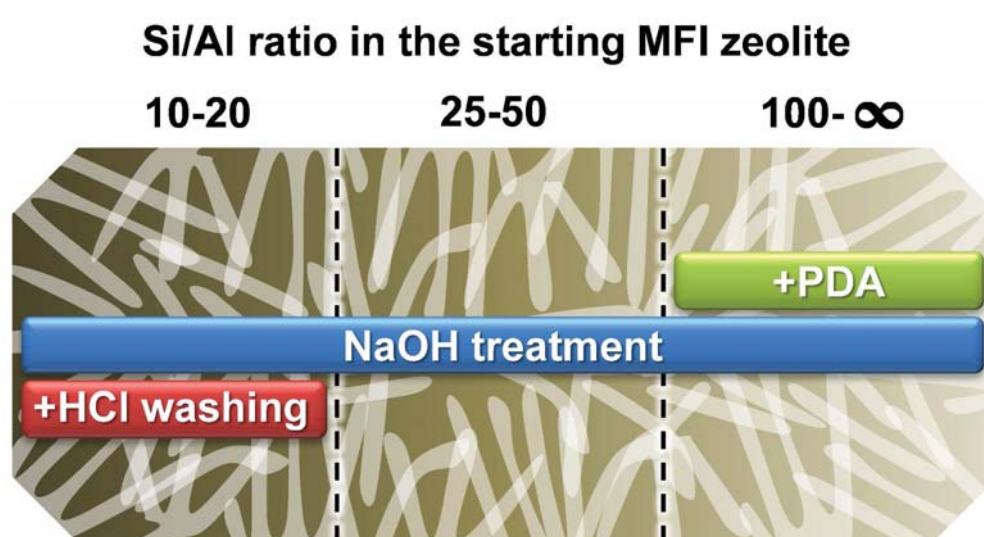


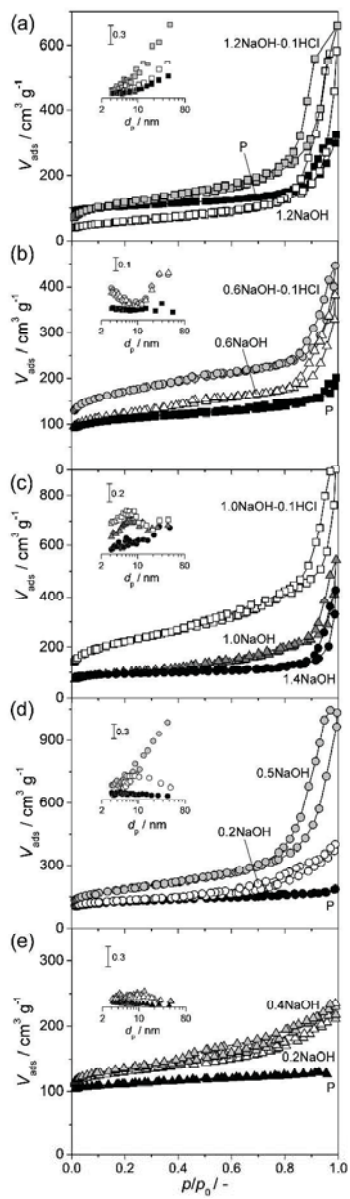
Figure 10



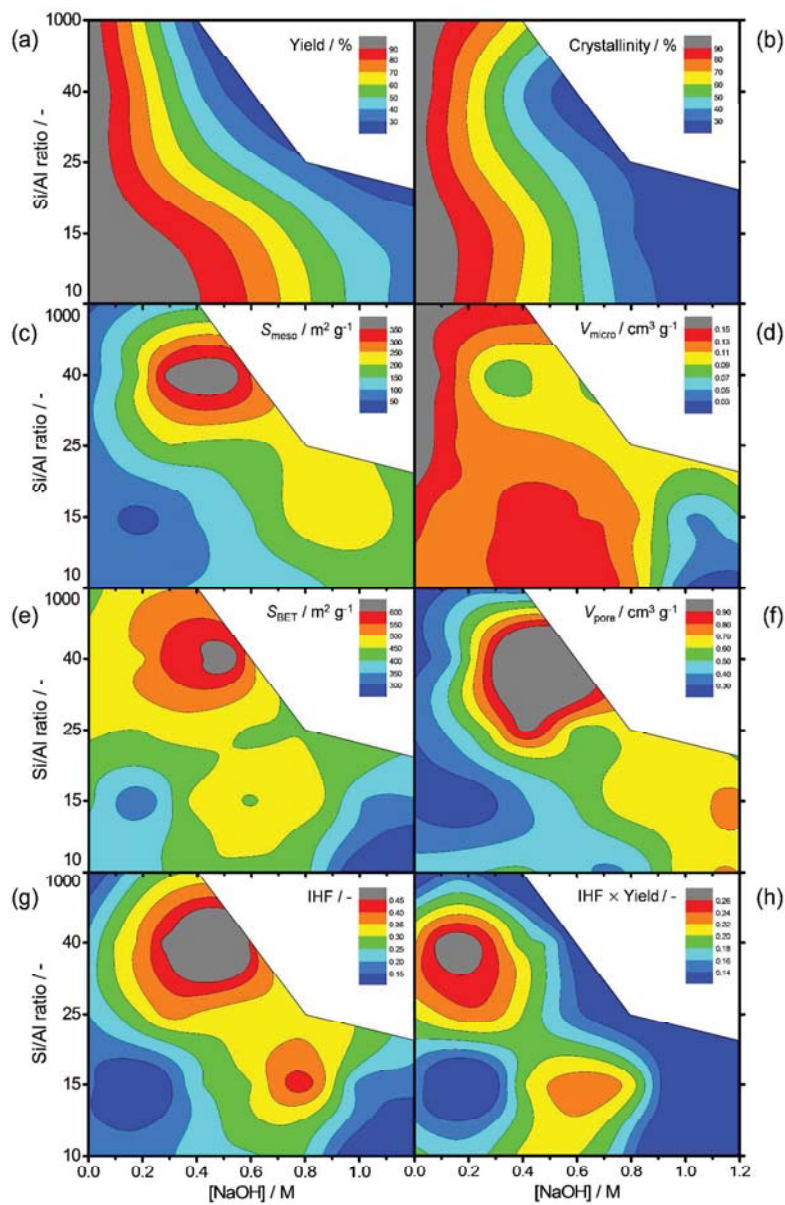
26
27
28
29
30
31
32
33
34
35
36
37
38
39
40
41
42
43
44
45
46
47
48
49
50
51
52
53
54
55
56
57
58
59
60

Desilication in alkaline medium is a suitable post-synthetic method to prepare hierarchical porous MFI zeolites independent on the Si/Al ratio in the parent material. Mesoporosity introduction in Al-rich zeolites requires sequential alkaline and acid treatments. The sequential acid wash removes amorphous Al-rich debris, which restores acidity and further enhances the porous and catalytic properties.

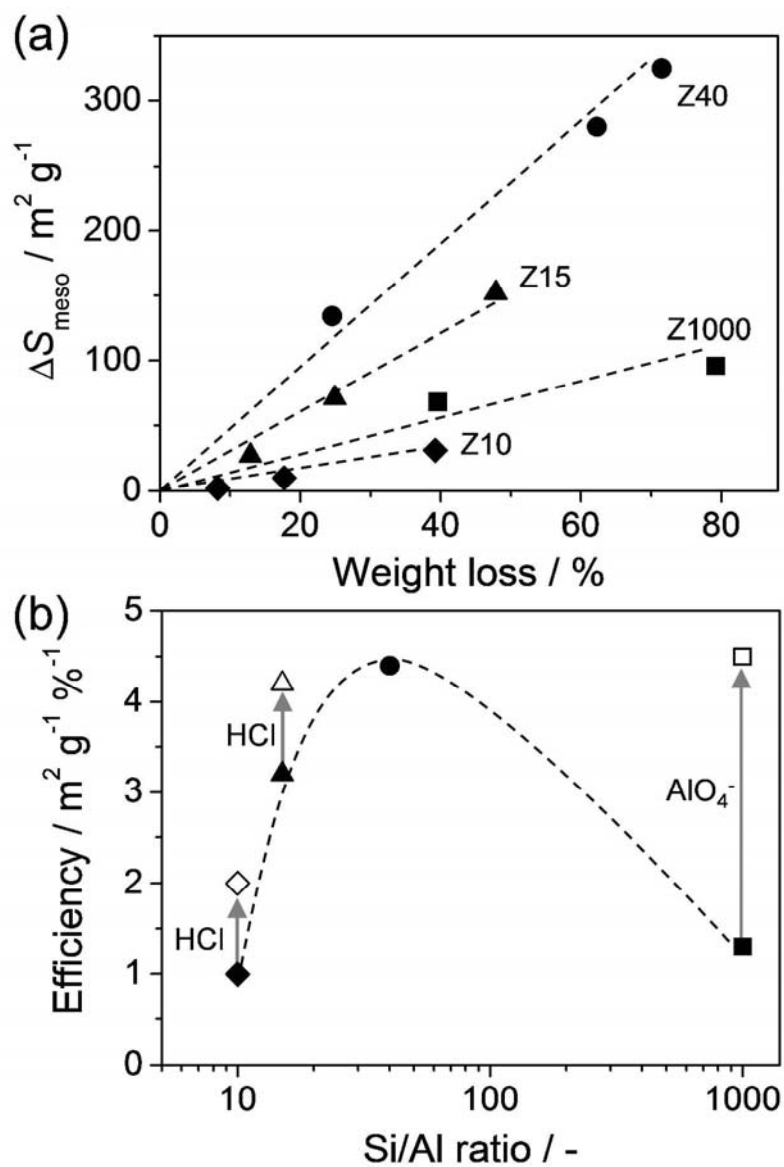
983x551mm (96 x 96 DPI)



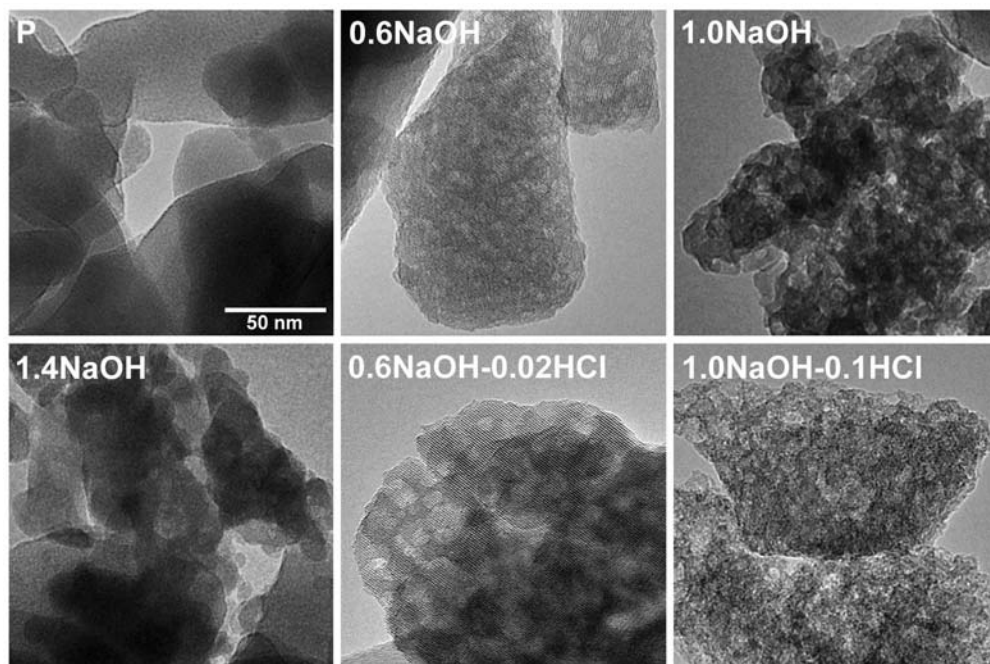
796x2494mm (96 x 96 DPI)



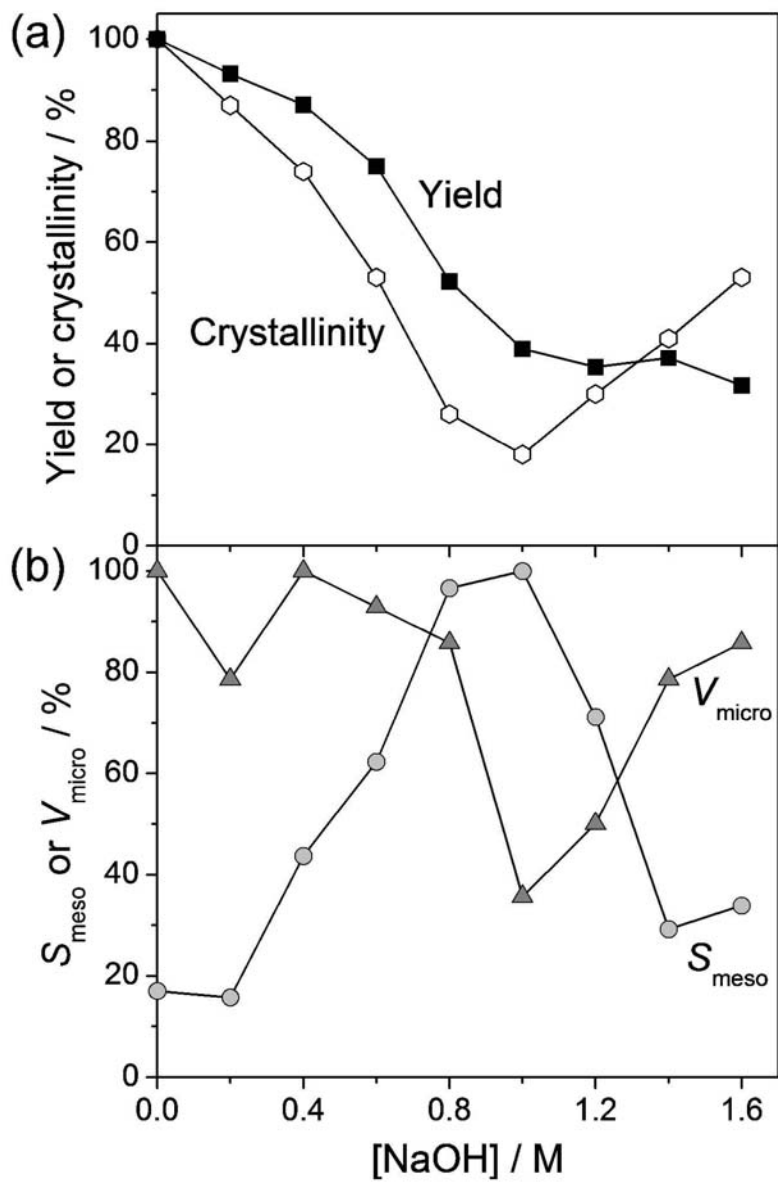
1077x1655mm (96 x 96 DPI)



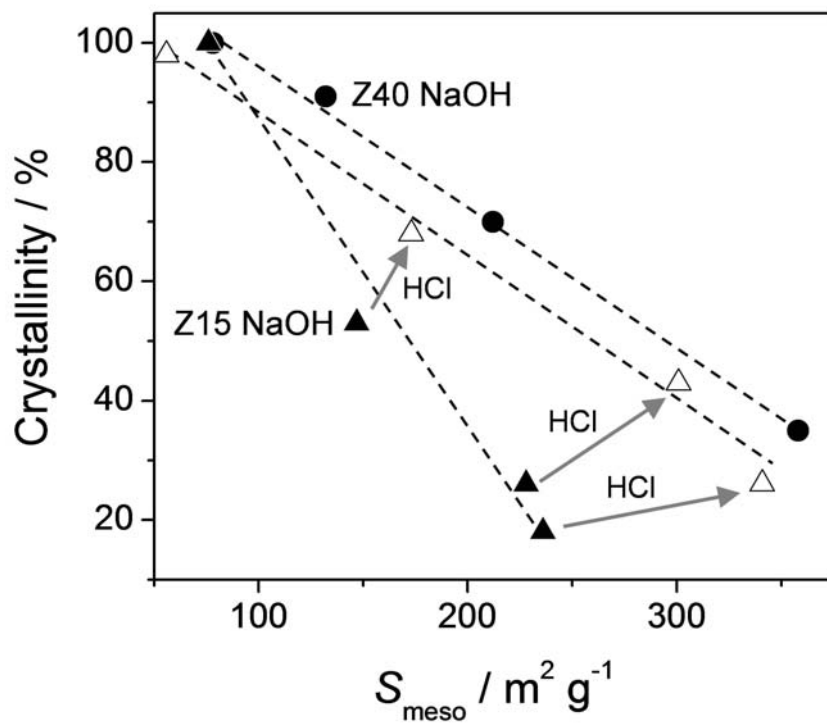
796x1044mm (96 x 96 DPI)



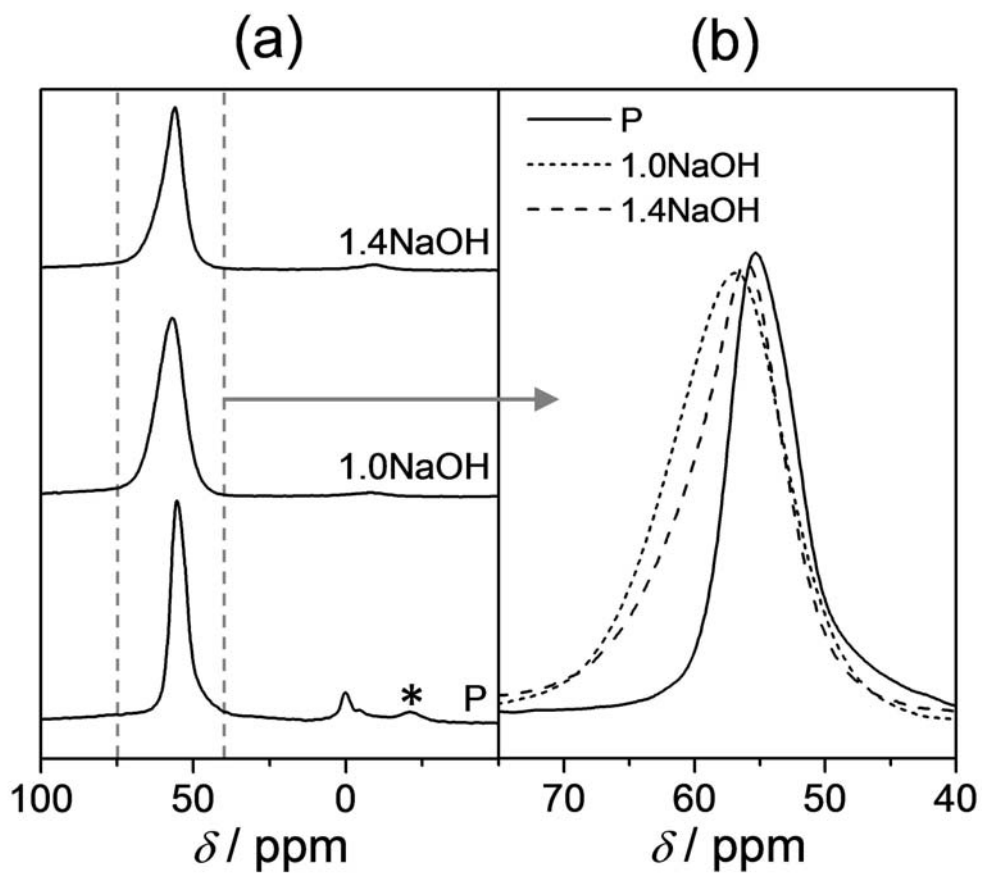
483x324mm (96 x 96 DPI)



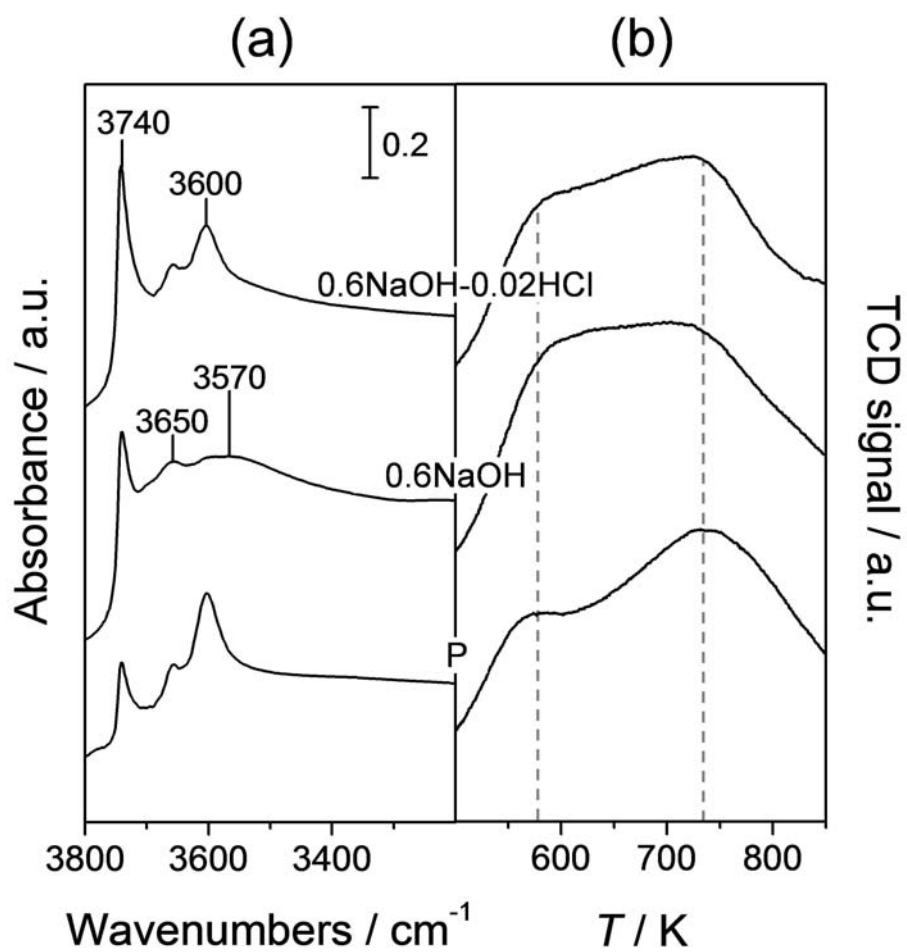
834x1070mm (96 x 96 DPI)



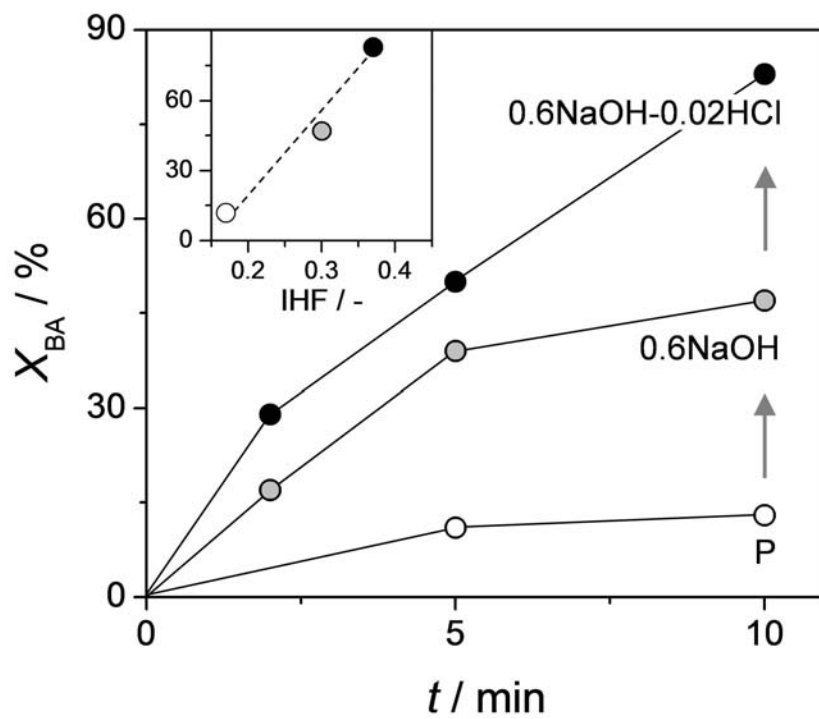
787x594mm (96 x 96 DPI)



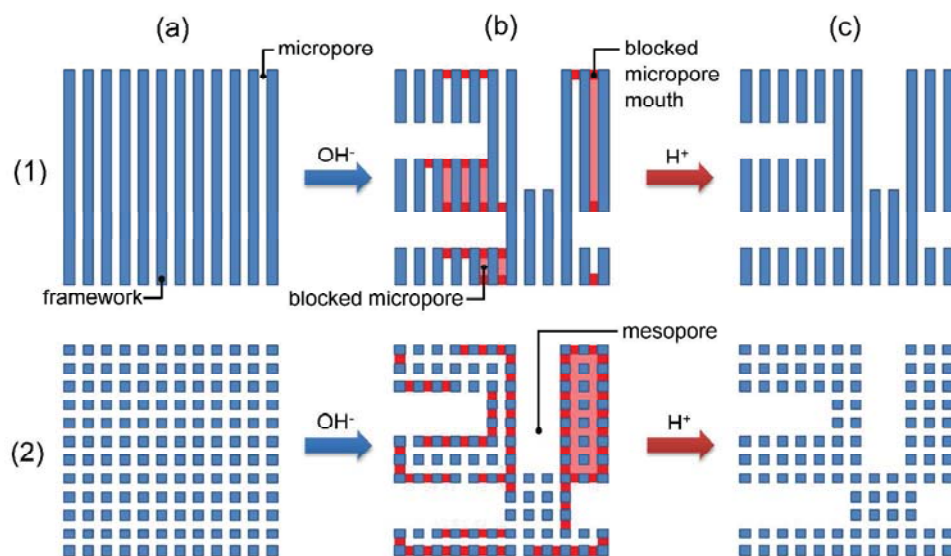
708x644mm (96 x 96 DPI)



777x792mm (96 x 96 DPI)



787x594mm (96 x 96 DPI)



1921x1078mm (96 x 96 DPI)